VTRC
Virginia Transportation Research Council

We Bring Innovation to Transportation

Computational Enhancements for the Virginia Department of Transportation's Regional River Severe Storm Model: Phase II

http://www.virginiadot.org/vtrc/main/online_reports/pdf/19-r24.pdf

MOHAMED M. MORSY, Ph.D.
Research Associate

YAWEN SHEN
Graduate Research Assistant

DANIEL VOCE
Undergraduate Research Assistant

GINA L. O'NEIL
Graduate Research Assistant

JONATHAN L. GOODALL, Ph.D., P.E.
Associate Professor

Department of Engineering Systems and Environment
University of Virginia

Final Report VTRC 19-R24

VIRGINIA TRANSPORTATION RESEARCH COUNCIL
530 Edgemont Road, Charlottesville, VA 22903-2454
vtrc.virginiadot.org

Standard Title Page - Report on Federally Funded Project

1. Report No.: FHWA/VTRC 19-R24	2. Government Accession No.:	3. Recipient's Catalog No.:
4. Title and Subtitle: Computational Enhancements for the Virginia Department of Transportation's Regional River Severe Storm Model: Phase II		5. Report Date: May 2019 6. Performing Organization Code:
7. Author(s): Mohamed M. Morsy, Ph.D., Yawen Shen, Daniel Voce, Gina L. O'Neil, and Jonathan L. Goodall, Ph.D., P.E.		8. Performing Organization Report No.: VTRC 19-R24
9. Performing Organization and Address: Virginia Transportation Research Council 530 Edgemont Road Charlottesville, VA 22903		10. Work Unit No. (TRAIS): 11. Contract or Grant No.: 111957
12. Sponsoring Agencies' Name and Address: Virginia Department of Transportation 1401 E. Broad Street Richmond, VA 23219	Federal Highway Administration 400 North 8th Street, Room 750 Richmond, VA 23219-4825	13. Type of Report and Period Covered: Final Contract 14. Sponsoring Agency Code:

15. Supplementary Notes:
This is an SPR-B report.

16. Abstract:

Climate change is projected to increase the risk of flooding, which can cause severe damage and threaten lives. This increased risk makes it even more important to accurately forecast potential flooding impacts. The report details efforts by the University of Virginia to enhance key aspects of the Virginia Department of Transportation's (VDOT) Regional River Severe Storm Model (R^2S^2) that aims to forecast potential flooding impacts in real-time for transportation infrastructure. This model serves as a planning tool for a large portion of the Hampton Roads District to assist residency administrators in efficiently allocating scarce resources to close roads and to assist first responders in accessing flood prone areas.

In this study, researchers first designed and implemented methods to improve the accuracy of R^2S^2 and reassessed the model against the stream data for two different storm events. The calibrated model shows good predictive capability for the majority of the study region, while the easternmost portion of the watershed, which has very flat terrain, remains the most difficult region to model accurately. The final task included automation of the cloud-based system that can provide end-to-end automation of flood warning for bridges and culverts in the region. The system is now available for implementation by VDOT for use during extreme weather events.

The study recommends that VTRC brief executives in the Department of Natural Resources on the work accomplished to date on R2S2. The briefing should include the capabilities of the current model, its current limitations, and potential modifications that could improve the model. In the spring of 2019, the Governor and the General Assembly determined that coordinated state agency research activities in the areas of climate change, sea level rise, roadway flooding attributable to storm surge, and roadway management strategies in flooding events are desirable. The Department of Natural Resources has been identified as the lead agency for these initiatives; the study's recommendation reflects that new interagency approach.

17 Key Words: Stormwater model, climate change, flooding forecasts		18. Distribution Statement: No restrictions. This document is available to the public through NTIS, Springfield, VA 22161.	
19. Security Classif. (of this report): Unclassified	20. Security Classif. (of this page): Unclassified	21. No. of Pages: 42	22. Price:

Form DOT F 1700.7 (8-72) Reproduction of completed page authorized

FINAL REPORT

COMPUTATIONAL ENHANCEMENTS FOR THE VIRGINIA DEPARTMENT OF TRANSPORTATION'S REGIONAL RIVER SEVERE STORM MODEL: PHASE II

Mohamed M. Morsy, Ph.D.
Research Associate

Yawen Shen
Graduate Research Assistant

Daniel Voce
Undergraduate Research Assistant

Gina L. O'Neil
Graduate Research Assistant

Jonathan L. Goodall, Ph.D., P.E.
Associate Professor

Department of Engineering Systems and Environment
University of Virginia

VTRC Project Manager
Bridget M. Donaldson, Virginia Transportation Research Council

In Cooperation with the U.S. Department of Transportation
Federal Highway Administration

Virginia Transportation Research Council
(A partnership of the Virginia Department of Transportation
and the University of Virginia since 1948)

Charlottesville, Virginia

May 2019
VTRC 19-R24

DISCLAIMER

ABSTRACT

Climate change is projected to increase the risk of flooding, which can cause severe damage and threaten lives. This increased risk makes it even more important to accurately forecast potential flooding impacts. The report details efforts by the University of Virginia to enhance key aspects of the Virginia Department of Transportation's (VDOT) Regional River Severe Storm Model (R^2S^2) that aims to forecast potential flooding impacts in real-time for transportation infrastructure. This model serves as a planning tool for a large portion of the Hampton Roads District to assist residency administrators in efficiently allocating scarce resources to close roads and to assist first responders in accessing flood prone areas. It represents a cutting-edge flood modeling system and could be implemented for other VDOT districts, once it is tested and refined for Hampton Roads District.

The specific project tasks described in this report were to (1) evaluate the current R^2S^2 based on real historical observations to access its accuracy; (2) enhance the model through calibration to improve its accuracy; and (3) automate the cloud-based flood warning system from end-to-end (forecasts to projected bridge impacts) so that it is able to provide timely information for the decision makers within VDOT.

In Task 1, the model was evaluated against stream data collected by the United States Geological Survey (USGS) for two storms and, based on this evaluation, a plan was designed and implemented to improve the model accuracy through the enhancement of key underlying datasets and calibration of model parameters. In Task 2, this plan to improve the model accuracy was implemented and the model was reassessed against the stream data for two different storm events. The calibrated model resulting from Task 2 shows good predictive capability for the majority of the study region, while the easternmost portion of the watershed, which has very flat terrain, remains the most difficult region to model accurately. In Task 3, the cloud-based system used to provide end-to-end automation of flood warning for bridges and culverts in the region was successfully automated. The system is now available for implementation by VDOT for use during extreme weather events.

The study recommends that VTRC brief executives in the Department of Natural Resources on the work accomplished to date on R2S2. The briefing should include the capabilities of the current model, its current limitations, and potential modifications that could improve the model. In the spring of 2019, the Governor and the General Assembly determined that coordinated state agency research activities in the areas of climate change, sea level rise, roadway flooding attributable to storm surge, and roadway management strategies in flooding events are desirable. The Department of Natural Resources has been identified as the lead agency for these initiatives; the study's recommendation reflects that new interagency approach.

FINAL REPORT

COMPUTATIONAL ENHANCEMENTS FOR THE VIRGINIA DEPARTMENT OF TRANSPORTATION'S REGIONAL RIVER SEVERE STORM MODEL: PHASE II

Mohamed M. Morsy, Ph.D.
Research Associate

Yawen Shen
Graduate Research Assistant

Daniel Voce
Undergraduate Research Assistant

Gina L. O'Neil
Graduate Research Assistant

Jonathan L. Goodall, Ph.D., P.E.
Associate Professor

Department of Engineering Systems and Environment
University of Virginia

INTRODUCTION

Climate change introduces significant challenges, especially for the low-relief coastal plain areas (Nicholls and Cazenave, 2010). These challenges include sea-level rise and the increased occurrence of extreme rainfall events (Sweet and Park, 2014). Severe flooding from extreme rainfall events can cause significant damage and threaten lives (Kates et al., 2006; Galarneau et al., 2013). Hurricanes Florence, Irma, and Harvey, which recently affected coastal area in North Carolina, Florida, and Texas, respectively, are examples of high return period rainfall events that have caused significant impacts. Infrastructure is vulnerable to the increase of extreme rainfall events (Schreider et al., 2000); however, there is little information about how these extreme rainfall events affect the integrated transportation system (Suarez et al., 2005). There is a need to accurately and quickly project potential flooding from forecasted rainfall events. This will allow decision makers to take steps to maximize the safety and minimize damages to the transportation infrastructure including bridges and culverts (Morsy et al., 2018; Sadler et al., 2018).

This report describes a project recently completed by the University of Virginia aimed at accomplishing key enhancements to the Virginia Department of Transportation's (VDOT) Regional River Severe Storm Model (R^2S^2). This model serves as a planning tool to assist VDOT residency administrators in efficiently allocating scarce resources to close roads and to assist first responders with accessing flood prone areas. It represents a cutting-edge flood modeling system that is ready to be implemented by VDOT for the project study domain, a portion of the Hampton Roads District.

This study builds on a prior study completed for VTRC, referred to in this report as Phase I of the project (Morsy et al., 2017). A key recommendation of Phase I was to determine the accuracy of the flood predictions derived from a version of the R^2S^2 model that was speeded up 50 times faster in Phase I by using a Graphical Processing Unit (GPU) solver. As part of this accuracy assessment, the Phase I final report recommended that the model be further calibrated to ensure that it produces accurate and actionable outputs for VDOT decision makers. A second recommendation of this prior study was to further automate data exchanges internal to R^2S^2 to streamline data processing tasks and make the system a fully automated flood forecasting system. This study, referred to as Phase II, aimed to address these recommendations in order to produce a version of the flood forecasting model that can be implemented by VDOT for decision making during extreme weather events. Throughout this process, the team communicated with VDOT's Hampton Roads District to ensure that modifications to R^2S^2 meet the district's needs.

METHODS

Purpose and Scope

The purpose of this research was to further improve the R^2S^2 model by addressing recommendations from Phase I of the project (Morsy et al., 2017). To achieve this goal, four tasks were completed in this Phase II of the project. Task 1 was to further evaluate the R^2S^2 model output for accuracy. Task 2 was to further calibrate the R^2S^2 model to improve its predictive accuracy for historical flooding events. Task 3 was to create new automated workflows internal to R^2S^2 so that the model can run end-to-end with minimal human intervention before, during, and after extreme weather events. Finally, Task 4 was to create this final report detailing the results of Phase II of the project.

Study Area

The study area is in the portion of the Chowan River basin that is within VDOT's Hampton Roads District, Virginia. The area is about 2,230 square miles (Figure 1), and includes the Nottoway River, the Blackwater River, and the Meherrin River. The longest flowpath according to the National Hydrography Dataset (NHD) is approximately 109 miles with a slope that varies from 0% to 21%. The study area includes 493 georeferenced VDOT bridges and culverts. Because a high portion of the study area consists of low-relief terrain, especially the easternmost portion of the study area, R^2S^2 uses a two-dimensional (2D) hydrodynamic model called Two-dimensional Unsteady Flow (TUFLOW) (Syme, 2001) (https://www.tuflow.com/). The area upstream of the project domain (2,010 square miles) consists of high-relief that can be adequately modelled using a spatially lumped hydrologic model. This upstream area is modeled using Hydrologic Engineering Center–Hydrologic Modeling System (HEC-HMS) to generate the inflow boundary conditions for the 2D domain when calibrating and evaluating the model using historical weather events. When run in a flood warning system mode, the National Water Model flood forecasting product replaces the HEC-HMS model to retrieve and generate the inflow boundary conditions for the 2D domain.

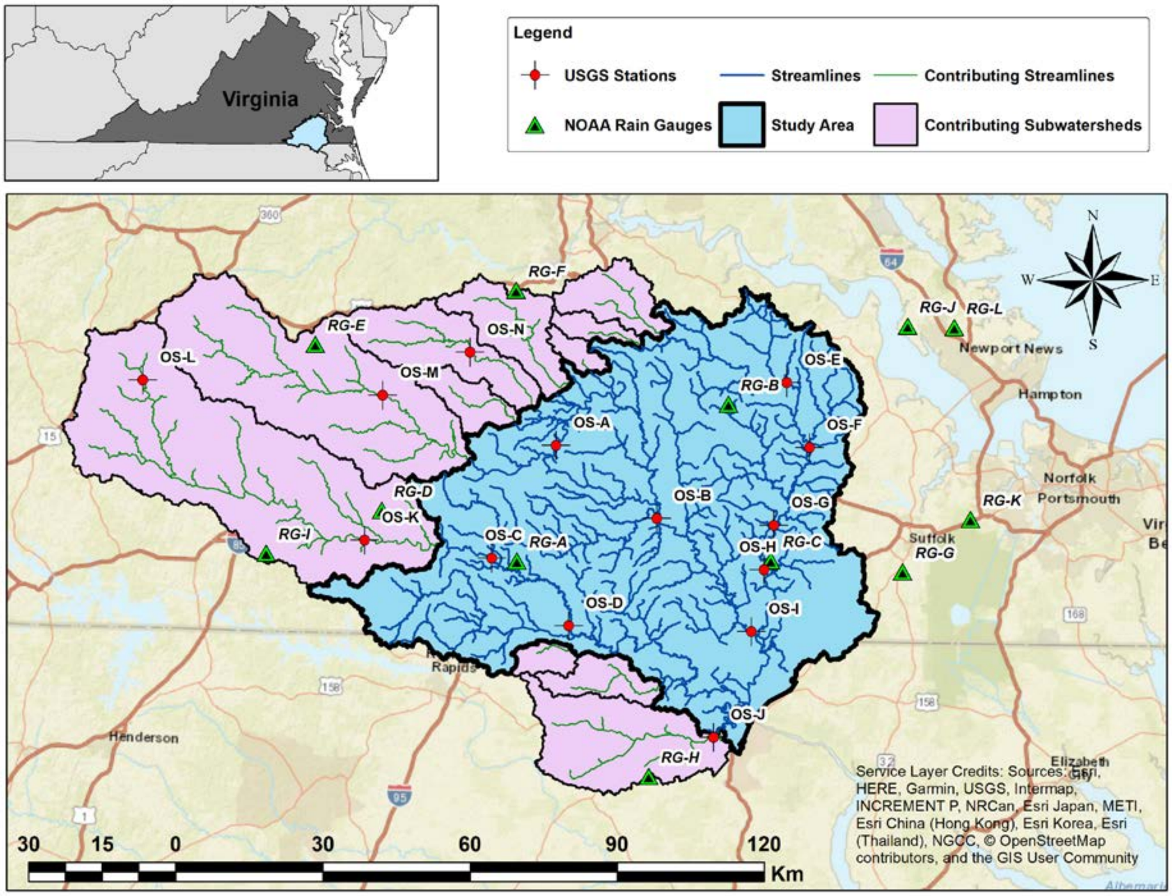

Figure 1. The study domain consisting of a 2D hydrodynamic model and 11 Subwatersheds that contribute the boundary inflow to the 2D model domain

Task 1: Model Evaluation

Prior to Phase II of this project, there was limited understanding about the accuracy of the R^2S^2 model. It was run for the Hurricane Sandy storm event with results that generally matched well with observed flooding at streamflow gauging stations. The R^2S^2 model had not been evaluated for other historical storm events in order to understand predictive accuracy and limits of the model's forecasting capabilities. These so called "hindcasts," where the computational forecasting model is run for historical storm events using the best available information for reconstructing these events, are important step in documenting the model's accuracy and utility as a decision support tool.

In Phase I of the project, an evaluation had been done to check the model accuracy between using different numerical solvers: TUFLOW CPU and GPU. Continuing this evaluation for Hurricane Sandy, in Phase II, the effect of changing the grid cell size and the Manning's coefficient values on the model results was investigated. Then, based on the outcomes from this investigation and the available observation data, another storm event, Hurricane Matthew (2016), was chosen that had a significant impact on the study area to evaluate the model performance before beginning the calibration process in Task 2.

Figure 1 shows the available USGS stations in the study area. By contacting USGS and with the help of a USGS employee (R. Russell Lotspeich), the available unpublished provisional water stage data for these stations were obtained. Table 1 shows the available water stage data for each USGS station. The data were cleaned-up and pre-processed to be compared with the 2D model outputs. TUFLOW has three different approaches to apply the rainfall to the computational cells. In Phase I, these approaches were explored and a decision made to use the gridded rainfall data with specific spatial and temporal resolution rather than the gauged rainfall data assigned to a fixed number of polygons covering the study domain. In this study, the direct rainfall data technique, using gridded rainfall data, was used to apply input rainfall values to every cell in the 2D hydrodynamic model. When the rainfall is directly applied to the cells, the model routes flow based on the cell topography on a cell by cell basis (Huxley and Syme, 2016). This is the same rainfall approach used in the flood warning system that was designed in Task 3 that uses the National Weather Service High-Resolution Rapid Refresh (HRRR) forecast rainfall data (Morsy et. al, 2017).

Table 1. USGS stations data availability in the study domain

ID	USGS Station	Stage Depth Data Availability	
		start	**End**
OS-A	**02045500** NOTTOWAY RIVER NEAR STONY CREEK, VA	10/1/2003	Current Date
OS-B	**02047000** NOTTOWAY RIVER NEAR SEBRELL, VA	10/1/2002	Current Date
OS-C	**02052000** MEHERRIN RIVER AT EMPORIA, VA	10/1/2003	Current Date
OS-D	**02052090** MEHERRIN RIVER NEAR BRYANTS CORNER, VA	11/26/2012	Current Date
OS-E	**02047500** BLACKWATER RIVER NEAR DENDRON, VA	10/1/2003	Current Date
OS-F	**02047783** BLACKWATER RIVER AT ROUTE 620 NEAR ZUNI, VA	4/25/2013	Current Date
OS-G	**02049500** BLACKWATER RIVER NEAR FRANKLIN, VA	10/1/2005	Current Date
OS-H	**02050000** BLACKWATER RIVER AT HWYS 58/258 AT FRANKLIN, VA	6/30/2010	Current Date
OS-I	**02047370** NOTTOWAY RIVER NEAR RIVERDALE, VA	7/11/2013	Current Date
OS-J	**02053200** POTECASI CREEK NEAR UNION, NC	10/1/1985	Current Date
OS-K	**02051500** MEHERRIN RIVER NEAR LAWRENCEVILLE, VA	10/1/2002	Current Date
OS-L	**02051000** NORTH MEHERRIN RIVER NEAR LUNENBURG, VA	10/1/2003	Current Date
OS-M	**02044500** NOTTOWAY RIVER NEAR RAWLINGS, VA	10/1/2003	Current Date
OS-N	**02046000** STONY CREEK NEAR DINWIDDIE, VA	10/1/2003	Current Date

The 2D hydrodynamic model's finite volume schemes are heavily dependent on the grid cell shape and size (LeVeque, 2002; Caviedes-Voullième et al., 2012). The TUFLOW model GPU solver uses only a Cartesian grid with the capability of changing the grid cell size. This allows parallelizing the computation on multiple GPUs. To assess the model performance with different grid cell sizes, the TUFLOW model was executed using the GPU solver with grid cell sizes of 50m (Original model grid cell size in Phase I), 40 m, 30 m, and 20 m. Then, based on the model results, the appropriate grid cell size was selected to optimize the model performance and execution time.

In addition to selecting the appropriate grid cell size, the Manning coefficient (n) was also adjusted throughout the model domain based on the land cover to test its sensitivity and ability to improve matching observed peak stages obtained from the six USGS stations. This is considered part of the evaluation process to inform the team on how this parameter affects the model results. The model initially had Manning coefficient values determined based on the study area land use. To assess the sensitivity of the model to changes in the Manning coefficient, this coefficient was changed to be a proportion of its original value: 0.6n, 0.8n, 1.0n, 1.4n, and 1.8n.

The model was tested on Hurricane Matthew, which had a significant impact on the study domain. Hurricane Sandy, which was originally used to develop the model, had a smaller impact on the study domain, even though it was one of the most destructive hurricanes to hit the east coast of the US. There were three additional USGS observation stations that recorded the impact of Hurricane Matthew than there were for Hurricane Sandy, making nine available USGS observation stations in total. The peak water level observed during Hurricane Matthew at most of the USGS stations was higher than the observed peak water level for Hurricane Sandy. Therefore, Hurricane Matthew was chosen for evaluating the current model status and used it for the calibration process. For the evaluation and calibration process, Google Cloud Platform (GCP) computational resources were used to run the model using the most powerful GPUs available at the time (4 GPUs NVIDIA P100). One run for hurricane Matthew takes about 10 hours using these powerful GPUs, making calibration of the model possible but still challenging.

The rainfall data from Hurricanes Sandy and Matthew were obtained from the Tropical Rainfall Measuring Mission (TRMM). This data, collected by satellites, has a resolution of 0.25 x 0.25 degrees, resulting in 16 cells covering the entire study area. Rainfall data from the Next Generation Weather Radar (NEXRAD) provided by NOAA was hoped to be used given its higher resolution, but there was no data available for the dates of Hurricane Sandy for the study area. This missing radar data can be due to scheduled maintenance at the radar sites, unplanned downtime due to severe weather, communications problems, or archive problems (NEXRAD, 2018).

The inflow boundary conditions from the upstream regions (sub-watersheds) of the 2D model domain were prepared for Hurricane Matthew using the HEC-HMS modeling software. Figure 2 shows the 2D model domain along with the structure of the HEC-HMS model for the sub-watersheds. In the HEC-HMS model, the runoff generated by rainfall inside the sub-watershed domain is calculated based on the SCS curve number. The hydrograph is determined by the Clark Unit Hydrograph method. When USGS stream stations are available upstream of the sub-watershed outlets, the outflow at the outlets is generated from two sources: (1) discharge routed from the upstream USGS station using the Muskingum routing method and/or (2) flow generated from the rainfall inside the sub-watershed (e.g., sub-watershed 29B). If no upstream USGS stream station is available, rainfall is used to drive the HEC-HMS model and predict outflow (e.g., 23B). Figure 3 shows the hydrograph generated at the outlet of the Subasin29B (39C in Figure 2) where USGS station OS-K is located as an example.

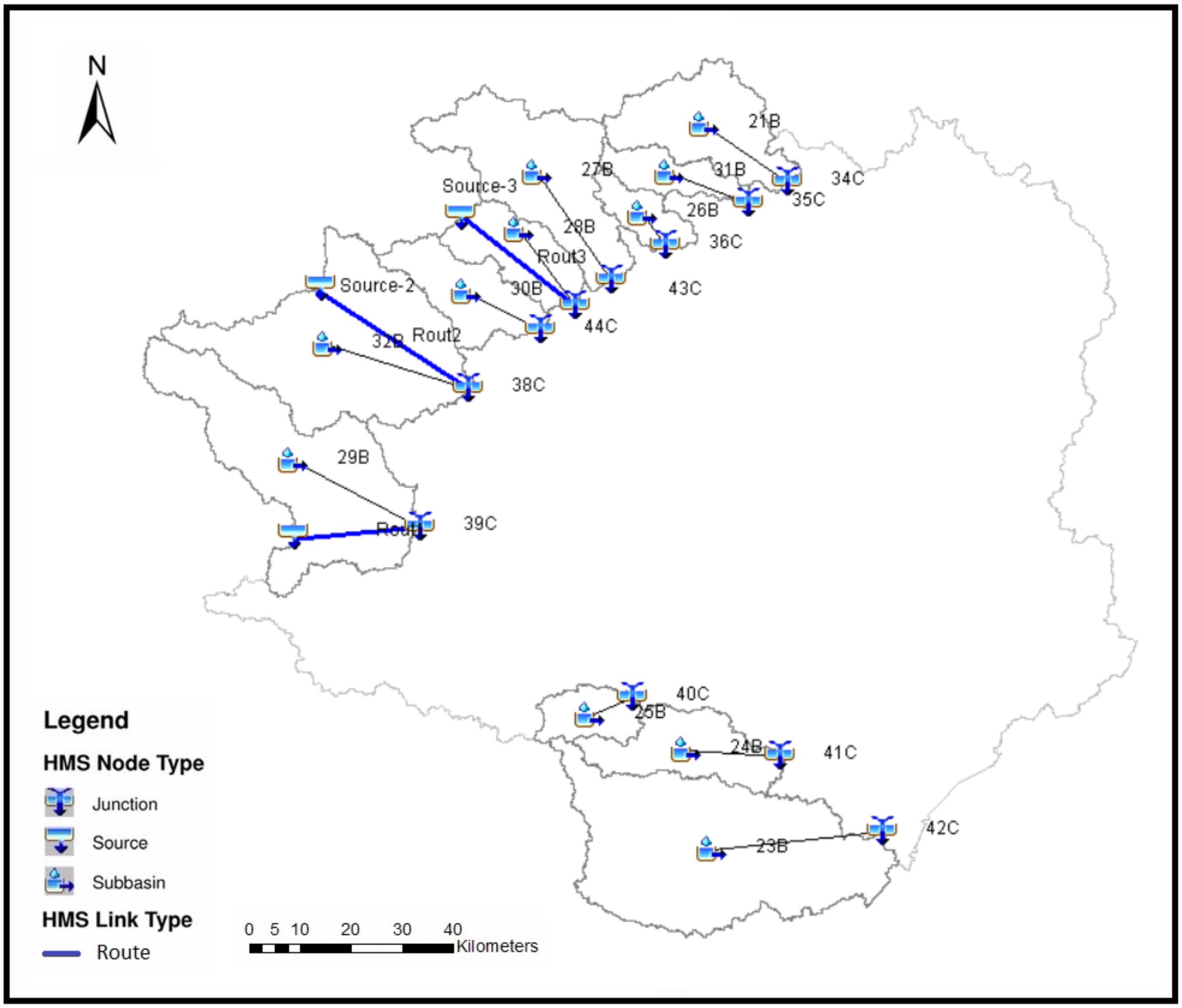

Figure 2. The HEC-HMS model components for the 11 subwatersheds that contribute the boundary inflow to the 2D model domain

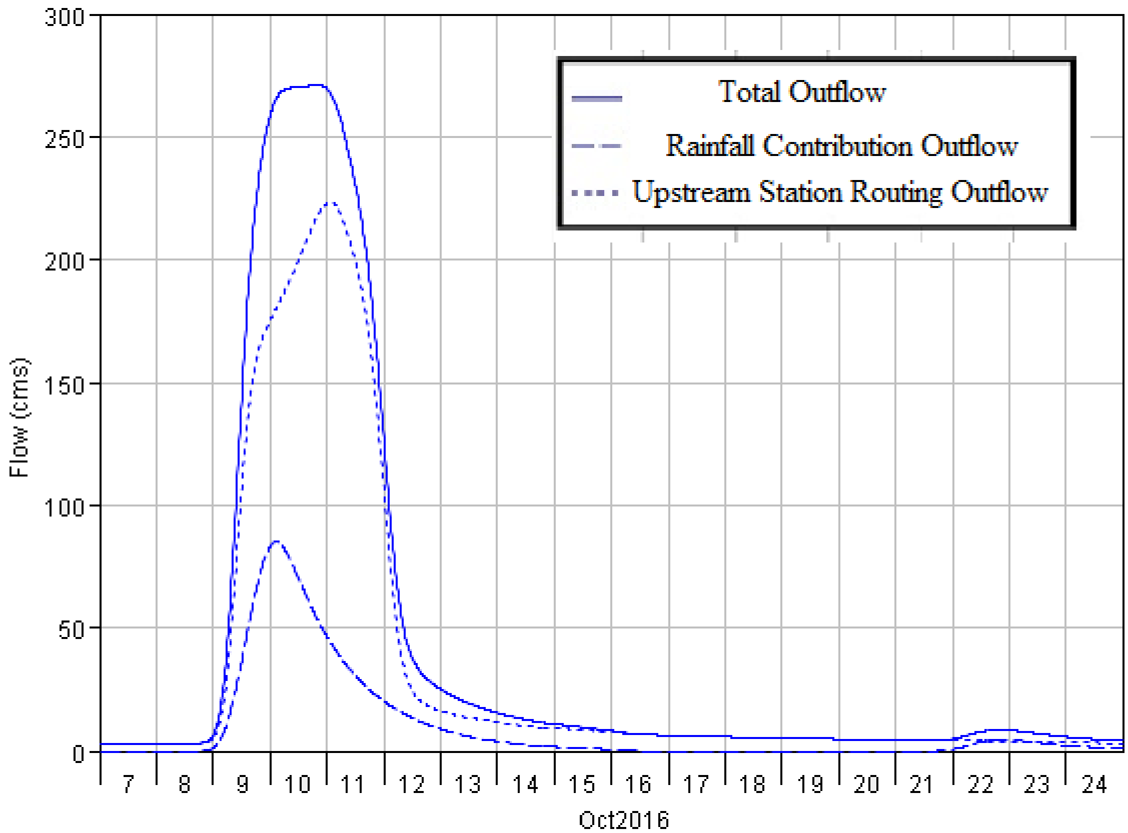

Figure 3. An example of the generated hydrograph combining the flow routing from USGS station OS-K and generated runoff at the Subbasin 29B

Task 2: Model Calibration

Given the limited available data, especially the scarcity of operating river gauges and available data for event-based calibration, it is a challenge to calibrate such a large study area. Model calibration is done in conjunction with model evaluation (Task 1) using well established best practices in hydraulic and hydrologic modeling (Refsgaard, 1997) so that decision makers can have confidence in the model results. In some instances, 2D models are not used due to the low resolution of the available spatial data and the difficulties of calibrating the model parameters (Caviedes-Voullième et al., 2012). A higher resolution digital elevation model (DEM) is required for 2D models due to the sophisticated approaches used to predict smaller hydraulic processes (Nicholas and Mitchell, 2003; Horritt et al., 2006). Additionally, it is important to identify the appropriate Manning's roughness coefficient, which has a significant effect on the 2D modeling results. There are available standard tables of Manning's values (Chow, 1959) that are considered a good way to assign the roughness in 1D models, but using these values directly with 2D models may not always be appropriate (Horritt et al., 2006). Also, roughness values may depend on the topography input data resolution, and the values change when the resolution changes.

Another challenge is the availability of the observation stream flow and stage data, which is compared to the model output to verify the model accuracy. As an example, this large study area includes only six USGS gauges that recorded Hurricane Sandy stream stage observation. Three of these stations are located on the same main stream in the eastern portion of the study area, one is in the middle of the study area, and the other two are located in the western part of the study area. More gauges with wider spread throughout the study domain would help improve the calibration of such a large 2D model. Therefore, in this task, the work focused on another more significant historical storm event to the study area, hurricane Matthew (2016), for which more USGS observation records were available. Because there were other storm events prior to Hurricane Matthew, an assumption was made about running the model with saturated initial conditions. Results of this step also highlight future opportunities for data enhancements that can be targeted in future work to further improve the accuracy of the model.

The model resulting at the end of Phase I had the following limitations: coarse resolution DEM, stream flowline with poor representation of reality, coarse resolution land use, and sparse rain gauge observation used for modeling historical storm events rather than using the gridded rainfall. Thus, during Phase II of this project, the main task for model calibration was focused on addressing these limitations by applying the following steps: 1) enhancing the model input by including the available higher resolution datasets and 2) conducting site visits to survey stream cross-sections for some bridges where USGS stations located at the low-relief east portion of the study domain. (This was conducted in addition collecting the bridges deck elevation. This information was a step to compensate for the lack of the bathymetry data.). Finally, step 3 included verifying the model outputs after applying the previous two steps by further investigating the applied rainfall datasets and methods. Final adjustments and model enhancements were also made to have the best calibration based on the current available resolution of the input data. These steps are detailed below.

Prepare and Pre-process High Resolution Input Datasets

In the first step, any available high-resolution data was considered, including higher DEM resolution, better representation of the stream flowlines, road network crossings at the main stream flowlines, and higher land use resolution. The gridded rainfall data was also considered rather than using just observation stations with a polygon method that lacks the spatial variability of the rainfall distribution. Figure 4 shows the main enhancements made to the input data for the model.

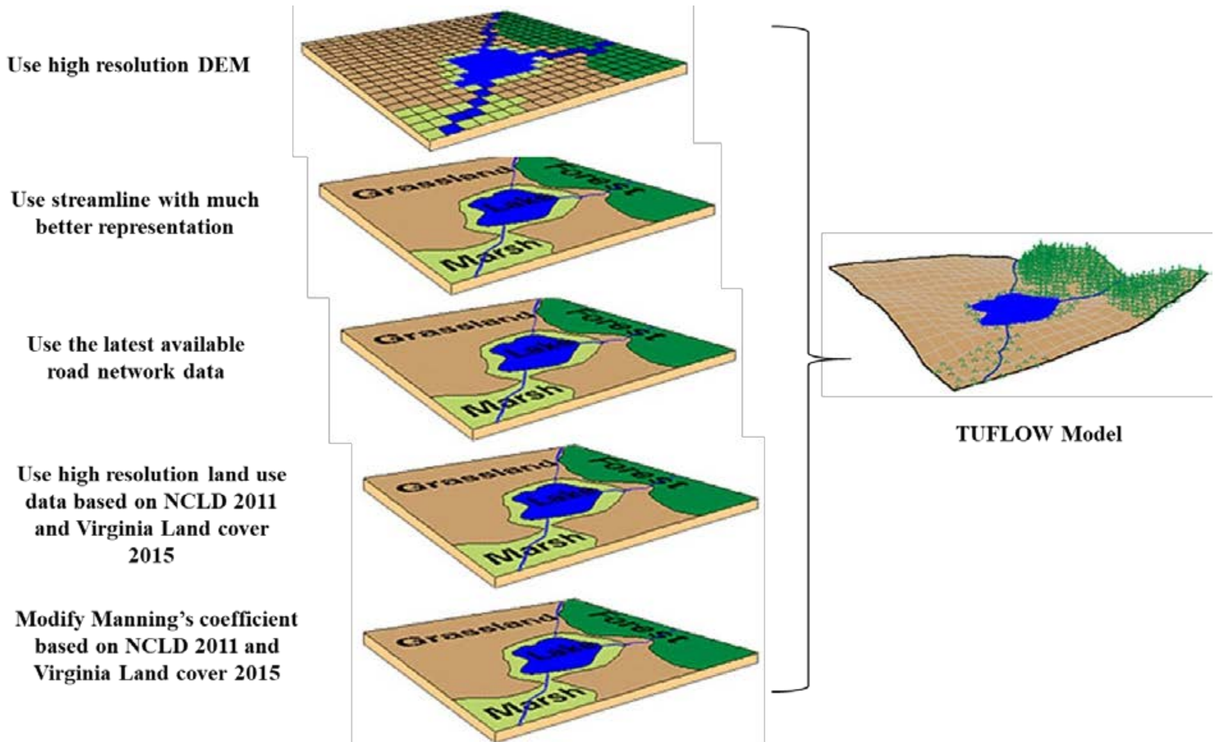

Figure 4. R^2S^2 flood warning model enhancements in Phase II

High Resolution DEM

The accuracy of the modeled stream flow is directly related to the accuracy of the topography data that is used and the available DEMs (Horritt et al., 2006). Light detection and ranging (LiDAR) systems are becoming commonly used as a remote sensing method to generate higher resolution floodplain topography for flood inundation modeling (Marks and Bates, 2000; Cobby et al., 2001). High resolution LiDAR data is available for the entire eastern portion of Virginia (Virginia LIDAR, 2018). The resolution of LiDAR data in Virginia varies from 0.76 m to 1.52 m, which is much higher than the resolution of the DEM used in the original version of the model (10 m). The LiDAR data is available for most of the study domain except for the western portion (as shown in Figure 5). The procedure to generate a high resolution DEM for the study region is provided in Figure 5. For areas where LiDAR data is available, the LiDAR data was resampled to 1 m DEM and all values were merged together. For the area where the high resolution LiDAR data was not available, the original 10 m DEM was kept but resampled to a 1m DEM and merged with the other processed high resolution LiDAR data. For this portion of the study area, using a DEM with 10m resolution is sufficient since the changes in the topography for the high relief terrains can be captured by the 10 m DEM resolution.

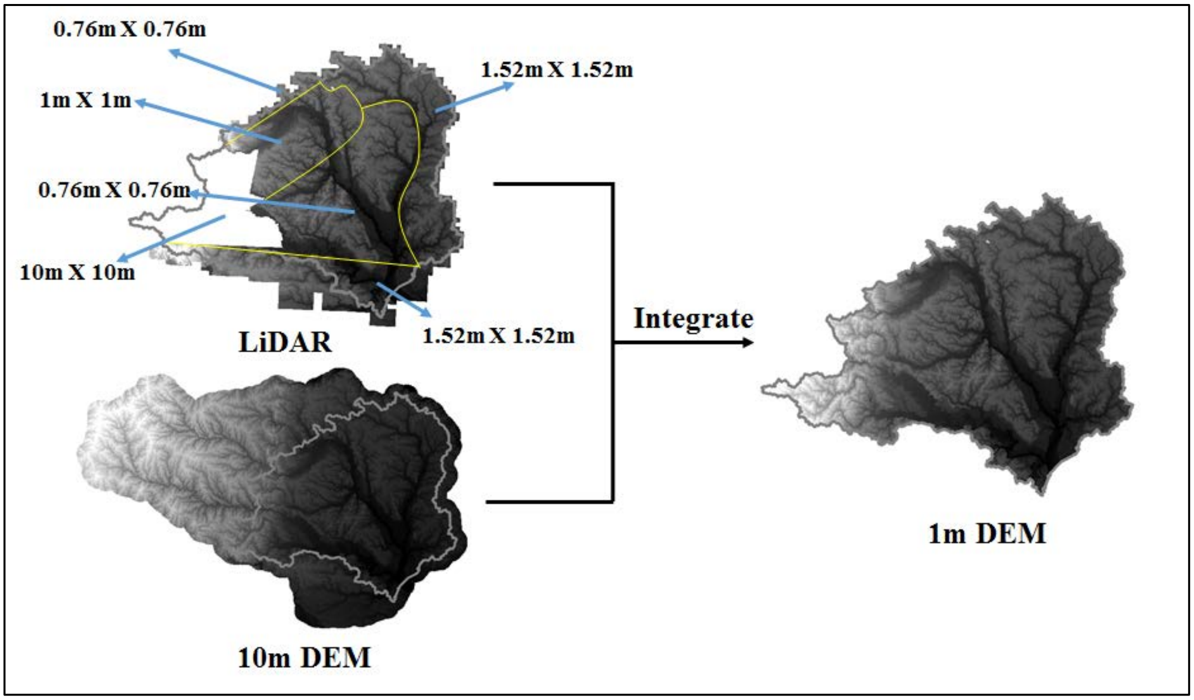

Figure 5. LiDAR availability in the study domain and the procedure to generate DEM with uniform cell size

Figure 6 shows a comparison between the original 10 m DEM and the new 1m DEM using a bridge cross-section in the study domain as an example. Overall, the cross-section at the bridge location from the 1m DEM is a better representation of the reality, and it also provides more detailed topographical features of the bridge cross-section.

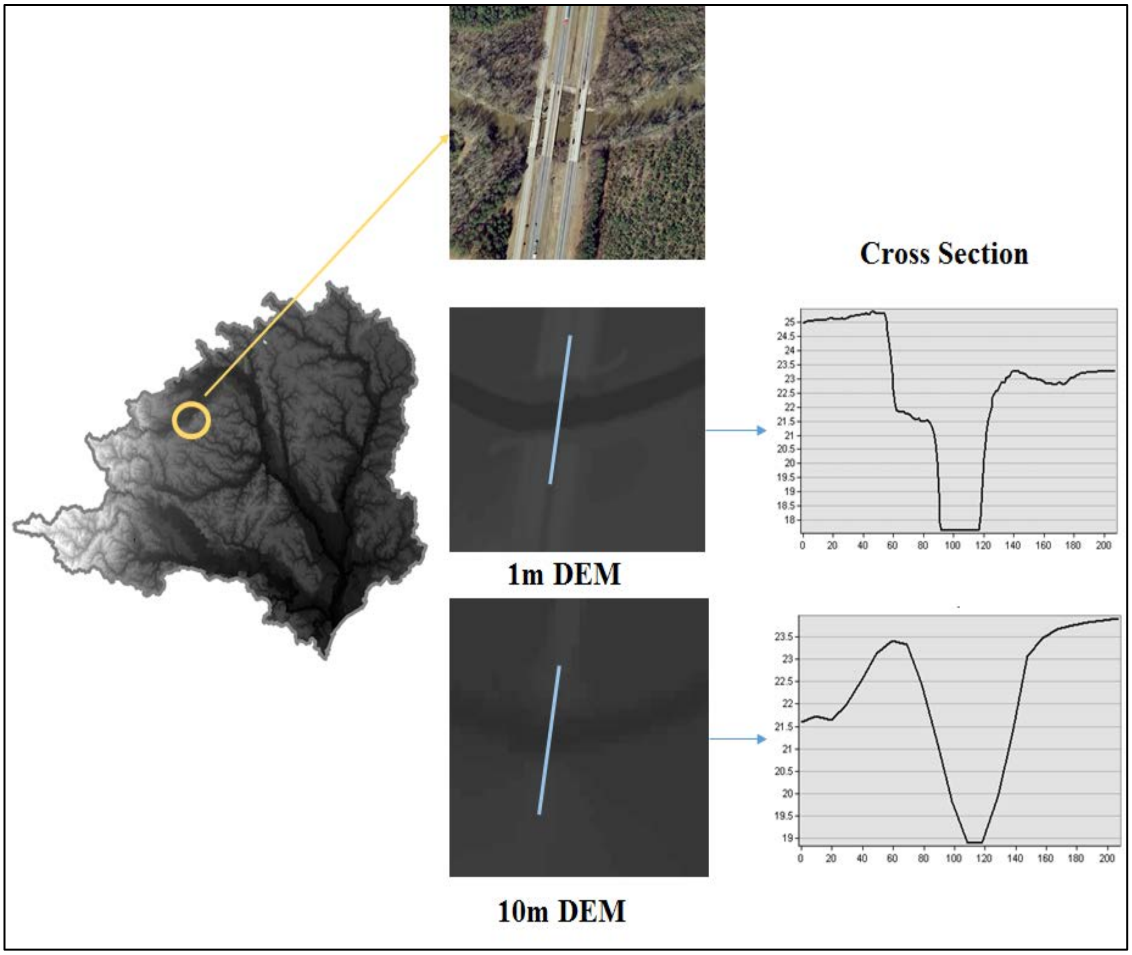

Figure 6. Comparison between the original 10m DEM and the new 1m DEM using a bridge cross-section as an example

Stream Flowline Modification

The stream flowline is one of the most important features in the 2D hydrodynamic model. The 2D model uses the stream flowline to define the clear passway for flow generated in 2D domain. A better representation of the stream flowline can greatly enhance the performance of the model. The original stream flowline represents the overall trend of the stream network, but it has several obvious errors. First, the stream flowlines do not align with the natural river for some locations in especially flat terrains. Second, some of the significant streams are not included in the streamline system. Third, some stream flowlines are not located at the center of streams. All these errors could reduce the accuracy of the model. To address these limitations, a new version of the stream flowline system was generated based on the latest available NHDPlus database (USGS, 2018). This stream flowline data has been modified manually to ensure the high quality of the stream flowline system and its alignment with the newly generated high-resolution DEM. The difference between the original and new version stream flowline representation is shown in Figure 7.

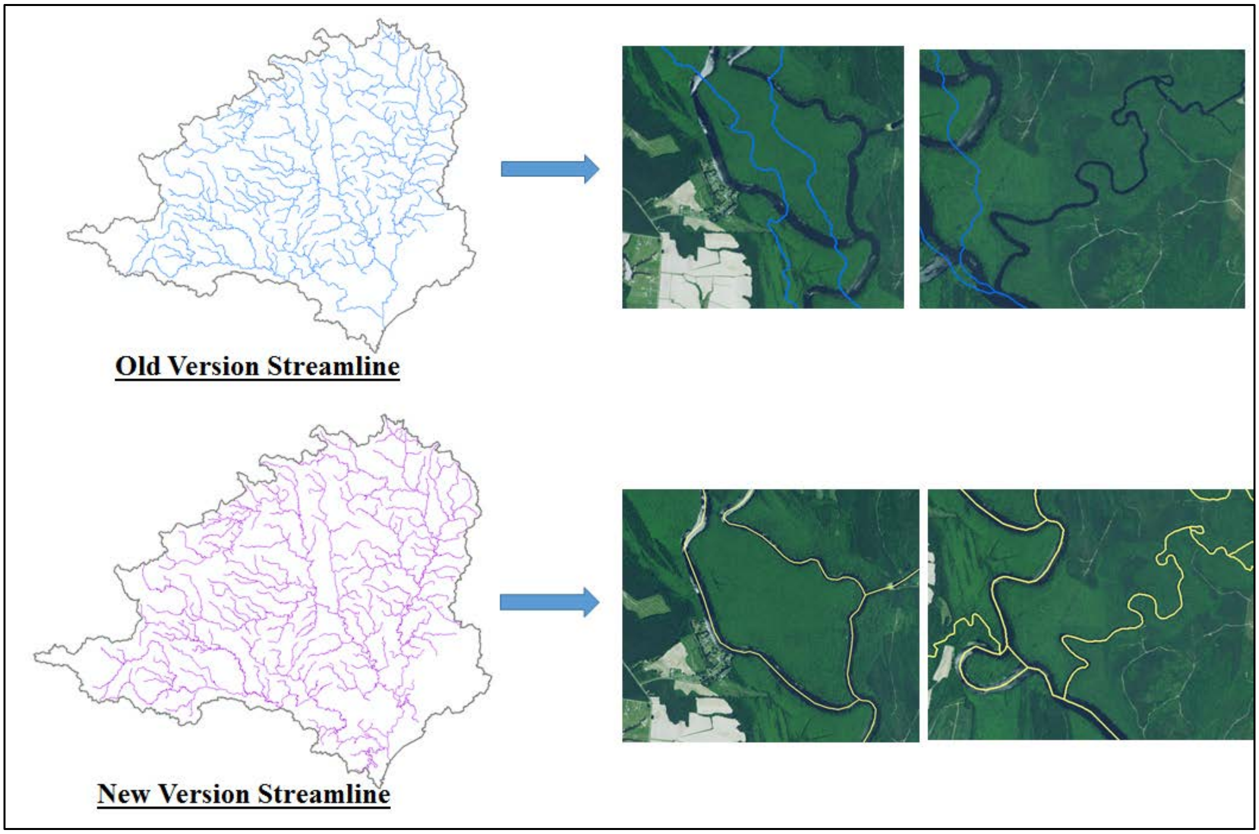

Figure 7. Streamline modified to have better representation of stream network

Road Network

In the 2D model, it is important to define the topography of the road network to mimic the reality of the overland flow and runoff. To represent the roads in the 2D model, the latest available centerline of the roads was used. This centerline data was obtained from the Virginia Geographic Information Network (VGIN) as indicator of the path of the road network, and survey points were extracted from the created high-resolution DEM to define the road elevations along this path. The new version of road network includes roads not only near bridge locations, but also across the entire floodplain (Figure 8). It was determined that it would be best to apply the road network only near bridge locations and across the floodplain (rather than across the entire study domain). If the entire road network is used, the model would treat roads as levees for the small stream tributaries that might be not represented in the stream flowline dataset. Therefore, the new version of the road network includes roads near bridge locations and across the entire floodplain but not throughout the study domain.

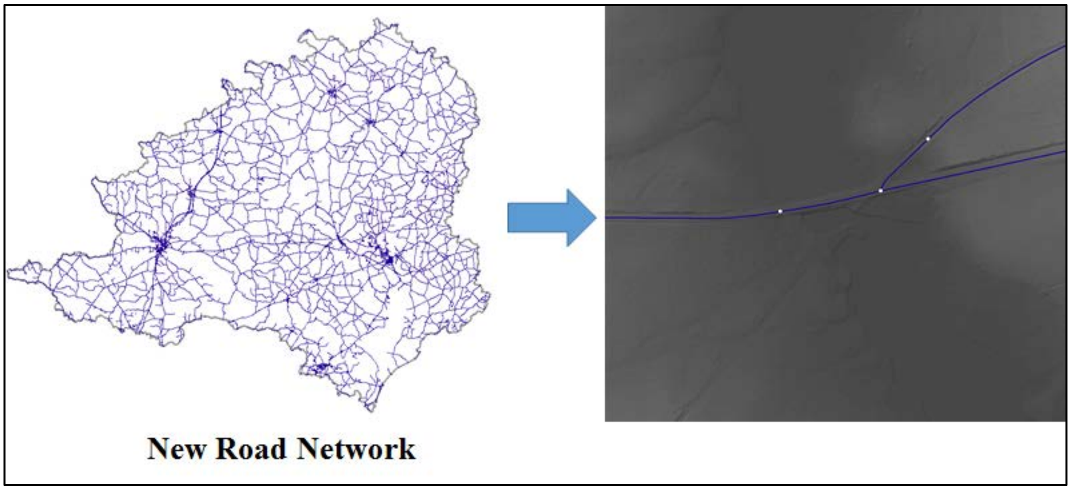

Figure 8. New version of the road network defined in the 2D model

Land Use and Manning's Coefficient

Manning's coefficient in the 2D model is defined by land cover maps. To have a better surface roughness representation, especially channel and floodplain roughness, two sources of land cover data with better spatial resolution were used to replace the original land cover in the previous version of the model. The first source is the National Land Cover Database (NLCD 2011: https://www.mrlc.gov/nlcd2011.php). The second source is the Virginia Land Cover Database (VLCD 2015), which is provided by VGIN (Virginia Geospatial Services, 2018). The NLCD 2011 has a spatial resolution of 30 m, and the VLCD 2015 has a spatial resolution of 3 m in the study region. The NLCD 2011 is used to define the Manning's roughness values for areas outside of the floodplain while the VLCD 2015 is used to define the Manning's coefficient within the stream channel and floodplain. Even though using the high resolution VLCD 2015 land cover map is more accurate, doing so for the entire study domain is problematic because it takes more than 10 minutes for the model to read the entire VLCD 2015 land cover map. Therefore, this high-resolution land cover map is only applied for the channel and floodplain to lower the model run time. The procedure to generate the land cover map for the TUFLOW model is shown in Figure 9. First, a 1 km buffer is created around the main streams. Second, the land cover map is extracted from VLCD 2015 underneath the 1km buffer. Finally, the extracted land cover map is merged with NLCD 2011. The Manning's coefficient defined for each type of land cover is provided in Table 2 and were taken from Kalyanapu et al., 2010. These values were used as initial values but further modifications were applied to them as part of the model calibration described in Task 3.

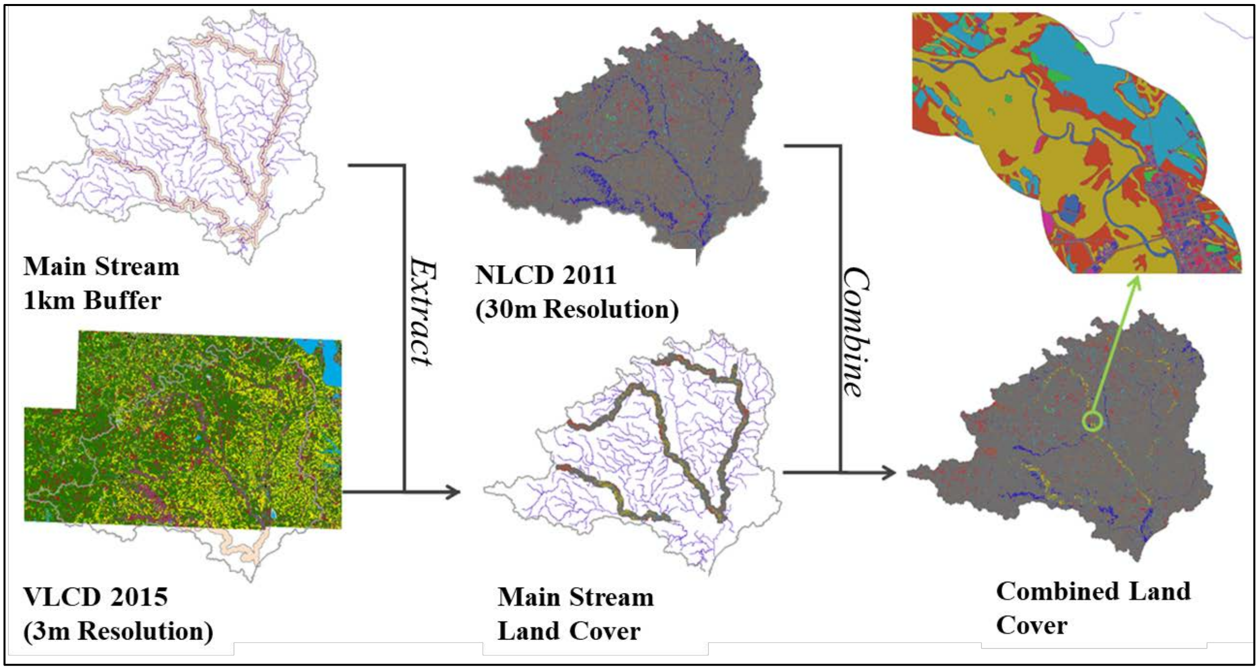

Figure 9. Procedure to merge National Land Cover Database 2011 and Virginia Land Cover Database 2015

Table 2. Manning's coefficients for different land cover types (Kalyanapu et al., 2010)

Land Cover Code	Land Cover Description	Manning's Coefficient (n)
11	Waterbody	**0.035**
21	Developed, open space	**0.040**
22	Developed, low intensity	**0.068**
23	Developed, medium intensity	**0.068**
24	Developed, high intensity	**0.040**
31	Barren land	**0.011**
41	Deciduous forest	**0.360**
42	Evergreen forest	**0.320**
43	Mixed forest	**0.400**
52	Shrub/scrub	**0.400**
71	Grassland/herbaceous	**0.368**
81	Pasture/hay	**0.325**
82	Crop/vegetation	**0.323**
90	Woody wetlands	**0.086**
95	Emergent herbaceous wetlands	**0.183**

Conducting Site Visits

For the second step, site visits were conducted, particularly focusing on the low relief area in the eastern portion of the model domain, which includes the Blackwater River that has a lack of bathymetry data. During these visits, cross section information and bridge deck elevation were collected where the USGS stations are located. This collected data was compared to the high-resolution DEM that was created, and the streamflow line evaluation points were adjusted accordingly to improve the model accuracy. All the USGS stations on the east portion of the model were visited (OS-E, OS-F, OS-G, OS-H, and OS-I). Figure 10 shows an example of collected cross sections upstream and downstream of the USGS station OS-H and the bridge 0871972-000000000029234 that were located at 36.68044, -76.9183.

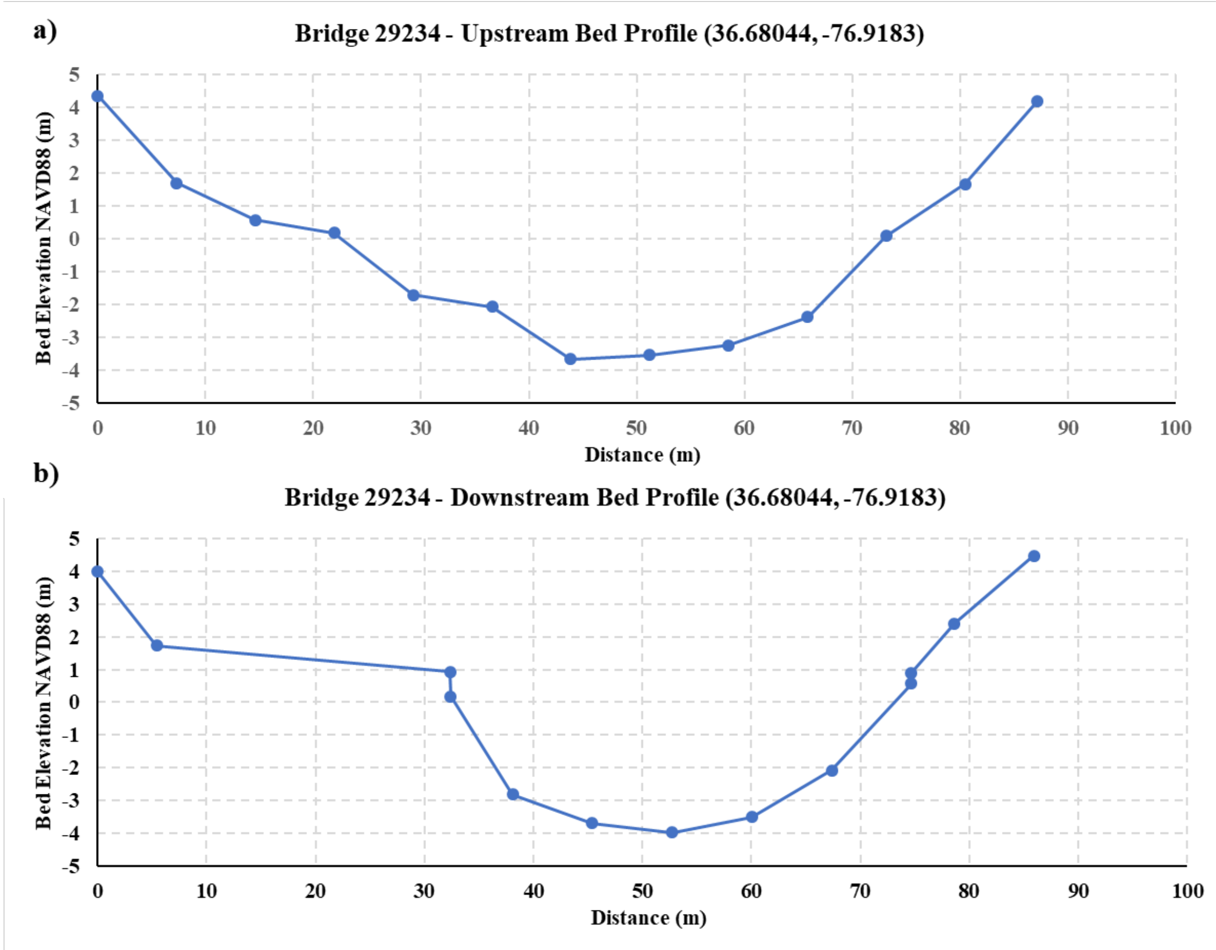

Figure 10. An example of the a) upstream, and b) downstream cross section at the USGS OS-H collected during the site visit

Further Enhancement to the Model

After comparing the modeled and observed stage depth at the USGS stations, there was a suspicion that there might be missing runoff volume. Therefore, for the final step, the gridded rainfall data from TRMM was compared with gauged rainfall data before making any further adjustments to the model parameters. This was accomplished by collecting the recorded rain gauge data available from 12 NOAA gauges (Table 3), which was used as inputs to generate model output; this model output was compared to the model output from using the TRMM gridded rainfall data. This was done due to the coarse spatial (0.25 x 0.25 degrees) and temporal (3 hr) resolution for the gridded rainfall data that is available for hurricane Matthew. The gauged rainfall data was collected for the duration of Hurricane Matthew from the NOAA gauges, which have the complete rainfall data records for this storm. Then, by using an Inverse Distance Weighting (IDW) method available within the TUFLOW model, this rainfall data was converted to gridded rainfall data with higher spatial (500 x 500 m) and temporal resolution (~20 min). This was done to take into consideration the spatial distribution of the storm event. Then this data was applied to the model to verify the quality of the used gridded rainfall data used during Tasks 1 and 2.

Table 3. NOAA stations with the availability of Hurricane Matthew rainfall data for the study domain

ID	NOAA Stations	Rainfall Data Availability	
		start	End
RG-A	72027803704 EMPORIA-GRENVLE RGNL ARPT, VA	1/1/2006	Current
RG-B	72401993773 WAKEFIELD MUNICIPAL ARPT, VA	1/1/2006	Current
RG-C	72308313763 FRANKLIN MUNICIPAL-JOHN BEVERLY ROSE AIRPORT, VA	10/16/1994	Current
RG-D	72077799999 LAWRENCEVILLE BRUNSWICK MUNI, VA	6/25/2014	Current
RG-E	72401599999 ALLEN C PERKINSON BLACKSTONE AAF / FT PICKETT, VA	9/22/2003	Current
RG-F	72401493714 DINWIDDIE COUNTY AIRPORT, VA	1/1/2006	Current
RG-G	72400703719 SUFFOLK MUNICIPAL AIRPORT, VA	1/1/2006	Current
RG-H	72307993796 TRI-COUNTY AIRPORT, NC	1/1/2006	Current
RG-I	72411893797 MCKNBRG-BRUNWICK RGNL ARPT, VA	1/1/2006	Current
RG-J	72308793735 FELKER ARMY AIRFIELD, VA	11/1/1960	Current
RG-K	72049999999 HAMPTON ROADS EXECUTIVE AIRPORT, VA	5/3/2011	5/20/2018
RG-L	72308693741 NWPT NEWS/WIMBURG INTL APT, VA	1/1/2000	Current

Further enhancement and calibration were done for the model by refining the hydraulic features and parameters of the model like the Manning coefficient and stream flowline width based on the available imagery data for the study domain. As a second calibration check, the modeled flow data at the USGS stations were compared to the observations. This gave an indication of the current model status for modeling the stage depth and flow throughout the study domain.

Task 3: Workflow Automation

This task focused on further automating data flows internal to the R^2S^2 model and design of a cloud-based, real-time modeling system for a 2D hydrodynamic model. This is to support decision-makers in assessing flood risk in Hampton Roads District area. Amazon Web Services (AWS) was used to build the flood warning system prototype. The prototype includes cloud-based execution for the 2D hydrodynamic model with high spatial resolution input data, utilization of GPUs for model execution speed-up, and a web front-end for dissemination of results and model initiation. The system is designed to run automatically if an extreme weather event is forecasted and produce results in near real-time.

There are two main forcing data sources used as inputs to the system: 1) the gridded forecast rainfall data and 2) the inflow boundary conditions for the 11 sub-watersheds surrounding the study area. In Phase I (Morsy et al. 2017), the HRRR data was chosen as the source for the gridded forecast rainfall data to the flood warning system. This HRRR data is missing the real-time rainfall data that the system uses for the first running time step. Also, using the HEC-HMS to generate the inflow boundary condition for the study area during operation as a flood warning system would increase the uncertainty in the forecasts. To address these issues, a decision was made to benefit from data available through the National Water Model (NWM), a new federal modeling effort, for the study domain. Using the NWM data would reduce the uncertainty of using the HEC-HMS model to prepare the boundary condition for the 2D model. This is because the NWM conduct assimilation for its results with the available USGS stations.

The NWM was also used to obtain the missing real-time rainfall layer within the HRRR data to the system. This rainfall data is pre-processed and prepared as an input to the NWM.

The NWM is a multi-agency effort in collaboration with the academic community and sponsored by NOAA to improve river and flood forecasts (Maidment, 2017) (http://water.noaa.gov/about/nwm). A key component of the NWM is a model called Routing Application for Parallel Computing of Discharge (http://rapid-hub.org/) that was developed to operate on the 2.67 million NHDPlus catchments and uses parallel computing to solve the 1D Muskingum flow equations on this large river network (Maidment, 2017). The NWM has made large strides in providing flood forecasting information on a large scale. However, the coarse resolution of the NWM and the use of a 1D hydrological model may not be sufficient for low relief terrains, such the coastal plain of Virginia. Running the R^2S^2 flood warning system in conjunction with the NWM allows the system to automatically obtain and pre-process the inflow boundary condition from the 11 sub-watersheds whenever the flood warning system is initiated due to forecasts extreme weather conditions. Moreover, The NWM was also used to obtain and pre-process the real-time rainfall data automatically whenever the system starts. This real-time rainfall data was used along with the 18 forecasted rainfall layers for the upcoming 18 hours from the HRRR data. Scripts were written using the Python programming language to automatically retrieve and pre-process the real-time rainfall data that is required for the first-time step of running the TUFLOW model and the inflow boundary condition. These scripts prepared both datasets in the required format for the TUFLOW model.

In summary, the goal of this task was to deliver a system that can (a) constantly monitor weather conditions, (b) automatically trigger model runs when extreme weather is forecast, and (c) provide VDOT with timely and actionable information on potential impacts throughout the duration of the flooding.

RESULTS AND DISCUSSION

Task 1: Model Evaluation

The TUFLOW model was executed using the GPU solver with different grid cell sizes using 50 m (Original model grid cell size in Phase I), 40 m, 30 m, and 20 m. For Hurricane Sandy, the output data from each of these runs with different grid cell sizes was compared to the available observed data for hurricane Sandy at six of the USGS stations. This comparison also includes the model results from executing the model using the CPU solver with cell size of 50 m. The modeled peaks using the GPU solver with 50 m grid cell size were significantly higher than the observed data and the model peaks using CPU solver at four USGS stations (OS-A, OS-B, OS-C, and OS-E). However, at one of the USGS station (OS-H), the modeled peak using the GPU solver with 50 m grid cell size was significantly lower than the observed data and the modeled peak using the CPU solver. Finally, at another USGS station (OS-G), the modeled peak using the GPU solver with 50m grid cell size was almost the same as the model peak using the CPU solver; however, both the peaks were significantly lower than the observed data. The differences between the modeled and observed peak stages could be due to the original coarse DEM resolution (10 m) and the lack of adequate bathymetry data in the major rivers and tributaries. For all of the minor tributaries and some stretches of the main rivers, bathymetry had to be assumed because no bathymetry data was available for the whole study domain.

Decreasing model grid cell size improved the matching of observed peaks at four of the six observation sites. Therefore, a decision made to use a smaller cell size in the model application. The drawback of a smaller cell size is an increase in model execution time. Figure 11 shows the model execution time using the GPU solver with different grid cell sizes (50 m, 40 m, 30 m, and 20 m). Figure 11 also shows the Mean Absolute Error (MAE) generated from comparing the model output using a GPU solver with different grid cell sizes and the model output using the CPU solver with the 50 m grid cell size. Based on these results, the 30 m cell size was chosen since there is only a small difference in the results using the GPU solver with a 20 m grid cell size model and there is a significant increase in the model run time (2.8x from 10.2 hours to 28 hours for Hurricane Sandy).

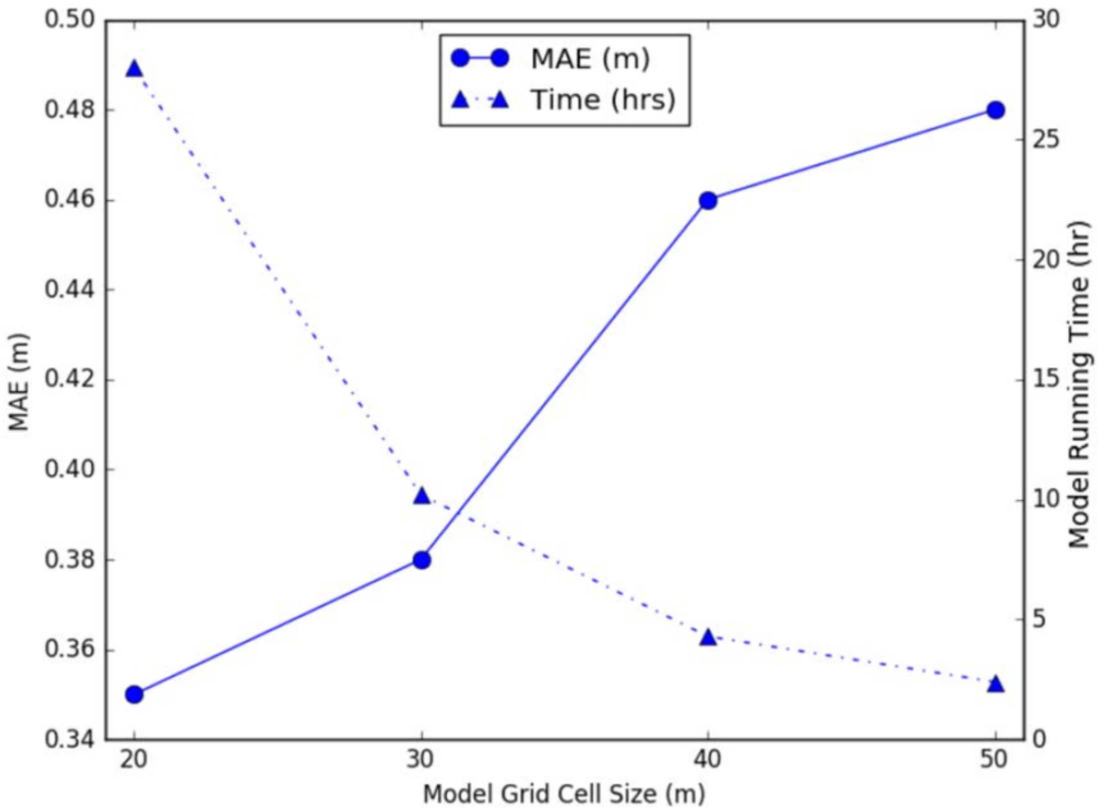

Figure 11. Model run time using GPU solver with different grid cell sizes and the corresponding MAE versus CPU solver (Morsy et al., 2018)

In addition to decreasing the grid cell size to 30m, the Manning coefficient was also changed to be 0.6n, 0.8n, 1.0n, 1.4n, and 1.8n of the original value. As the Manning coefficient value decreased, the modeled peak stages became closer to the observed peaks at stations OS-A, OS-B, OS-C, and OS-E. After reducing the grid cell size from 50 m to 30 m and the Manning's coefficient to 0.6n, the model came the closest to matching observed peak river stage. This represents a preliminary calibration of the model that was further investigated in Task 2.

Figure 12 shows the results of using the gridded rainfall data provided by TRMM for Hurricane Sandy when executing the model with grid cell size of 30 m and 0.6n using the GPU solver. Using the gridded rainfall data with this coarse resolution produces results very similar to those found when using the rainfall gauge data and the polygon method (Morsy et al., 2017). The model results nearly match the observation peaks at OS-A, OS-B, OS-C, and OS-E USGS stations. The other two USGS stations, OS-H and OS-G, where the modeled peaks are further from the observed peaks, are located on the same stream at the eastern portion of the study area along with Station OS-E. This area is the most low-relief terrains in the study domain. At OS-E station, the model predicts a slightly higher peak than the observed data and the modeled peak using the CPU model. The second station (OS-G) has a much lower peak than the observed data. However, the modeled peak using the CPU solver is even lower than the modeled peak using the GPU solver. The peak at station OS-H is much higher than the observed peak and the modeled peak using the CPU solver. The variation between the observed and modeled peaks at these three stations could be due to the coarse DEM resolution (10 m) used in the model. The slightly higher peak at OS-E may be due to slopes derived from the DEM being milder than the real slopes. The much lower peak and lower volume at OS-G could be due to having slopes derived from the DEM that are much steeper than the real slopes. Like with OS-E, the much higher peaks at OS-H may be due to the DEM-derived slopes, which are milder than the real slopes. This would explain why the absolute differences in the peaks at stations OS-G and OS-H are nearly the same, but the one is below and the other is above the observed peak. If the slopes of the contributing areas to station OS-G were milder, the peak there would be higher and the peak at the downstream station (OS-H) would be lower, making both closer to the observed data. This might improve if a higher DEM resolution is used within the model than what was applied in Task 2.

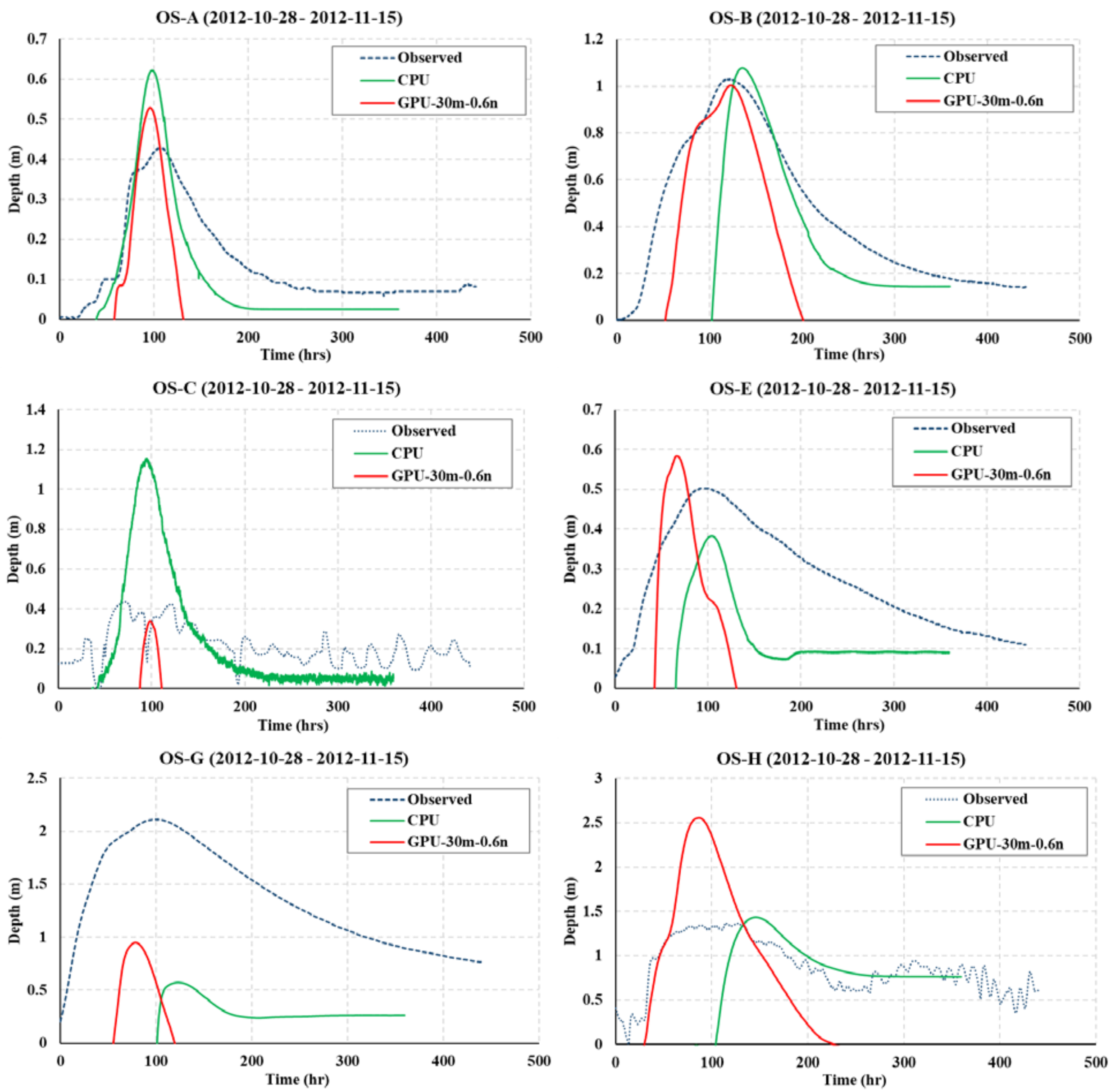

Figure 12. Comparisons between the observed stage depth data and the modeled depth generated from using a GPU solver with 30 m cell size and 0.6n Manning coefficient values (Morsy et al., 2018)

To test the model on another storm event with much more serious impact on the study domain, the model was tested on Hurricane Matthew (2016). The peak water level observed with Hurricane Matthew at most of the USGS stations was higher than that observed with Hurricane Sandy. Therefore, Hurricane Matthew was chosen for evaluating the current model status (with 30 m computational cell size) and it was used for the calibration process. The model was tested on Hurricane Matthew and the results were compared with water level observations from the nine USGS stations, as shown in Figures 13 and 14. Overall, the performance of the model was found to be much better than its performance with Hurricane Sandy. The results show a fairly good fit at stations OS-A, OS-C, OS-E, and OS-F. The model outputs captured the general trend of observation from station OS-B, OS-D, and OS-G. The model did not perform well at station OS-H and OS-I, possibly because these two stations are located on the flattest region of the study domain. It is very challenging to conduct flood modeling for this region due to the lack of topographic relief. For these reasons, in Task 2, further calibration work was done to enhance and improve the accuracy of the model.

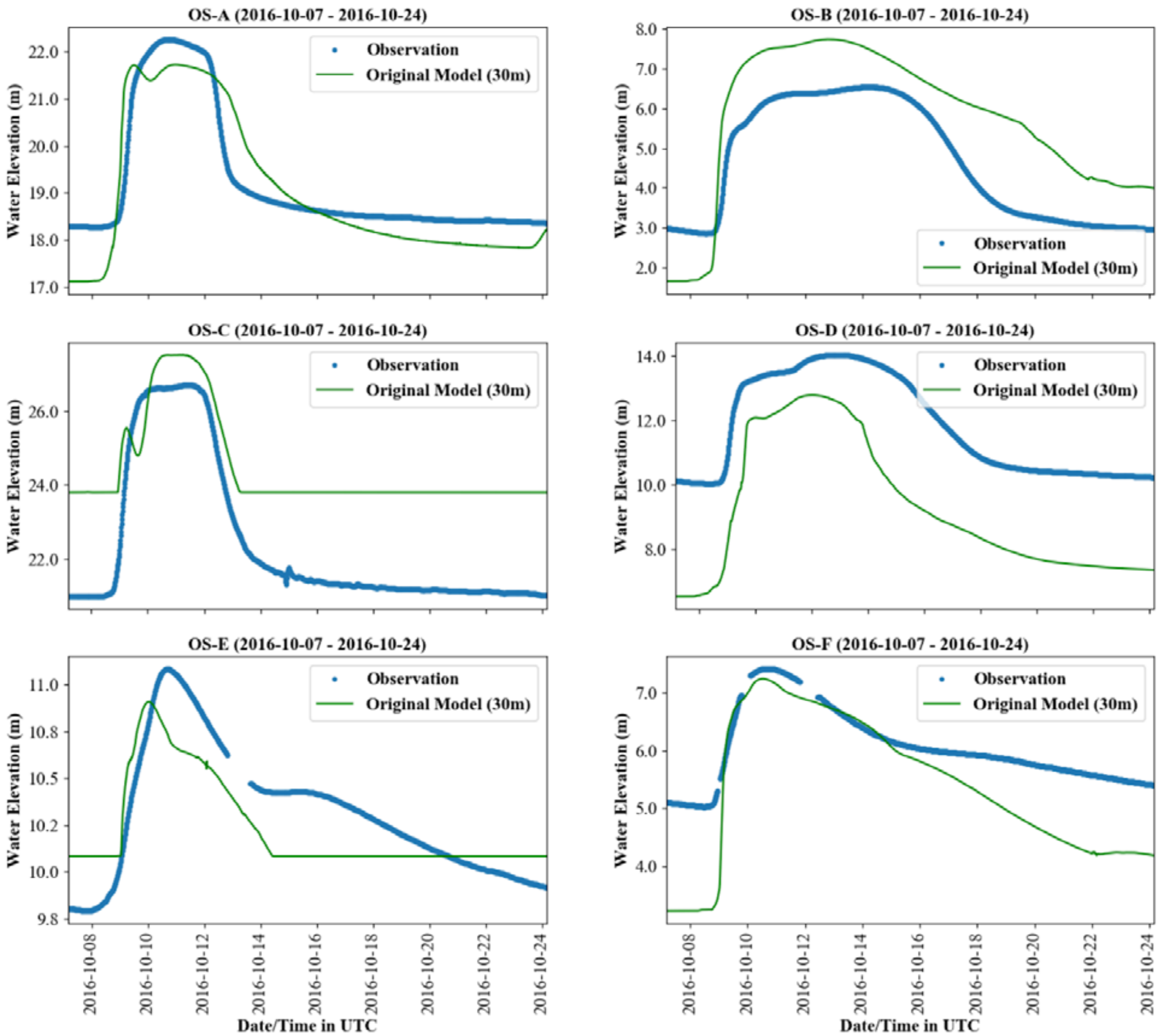

Figure 13. Model evaluation on Hurricane Matthew by comparing with USGS observations at OS-A, OS-B, OS-C, OS-D, OS-E, and OS-F

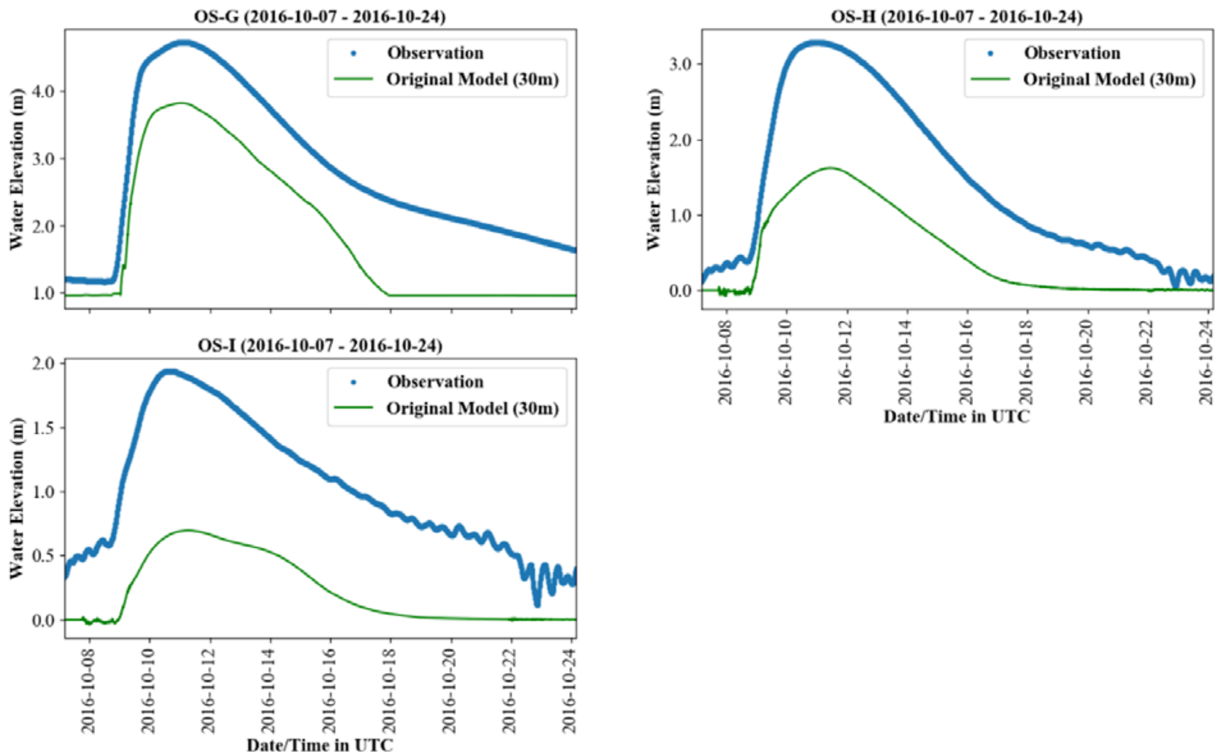

Figure 14. Model evaluation on Hurricane Matthew by comparing with USGS observations at OS-G, OS-H, and OS-I

Task 2: Model Calibration

In this task, the focus was on calibrating the model to address the limitations and inaccuracies of the model identified through Task 1. It was found that the most significant factors affecting the model performance were the DEM spatial resolution, the streamflow line representation and its consistency with the DEM, and the land use resolution with its corresponding Manning's coefficient.

After enhancing the model input by including the available higher resolution datasets described in the Methods section, the model outputs showed better fit with observations at the USGS stations OS-A, OS-C, OS-B, OS-D, OS-E, and OS-F (Figure 15). The initial water level from the current version of the model is much closer to the observed initial water level. As the most important factor for assessing the impact of flooding to bridges, the peak water level simulated from the calibrated model is much more accurate at most of the USGS stations.

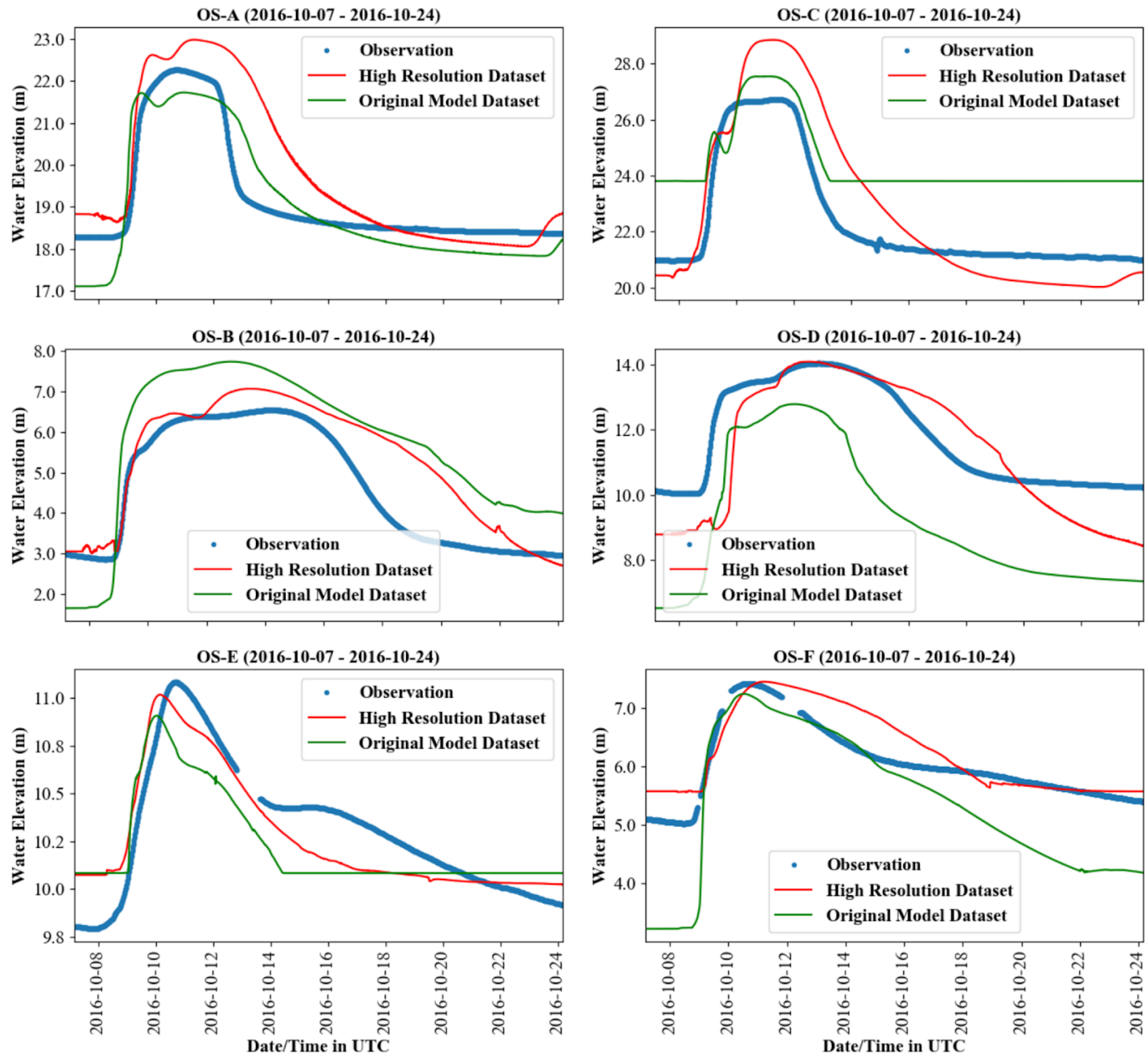

Figure 15. Model output for Hurricane Matthew before and after the high resolution inputs was implemented at USGS stations OS-A, OS-C, OS-B, OS-D, OS-E, and OS-F

However, the model still had poor accuracy at the three stations located on the southeast portion of the model, as shown in Figure 16, which is the flattest region in the study domain. Due to the lack of reliable bathymetry or river cross-section survey in this region, it is difficult to define the correct geometry features of rivers, i.e., river bed elevation and width. The historical cross-section survey for some bridges in this region was provided by VDOT (specifically by John H. Matthews). Also, the bridge cross-section was surveyed for this region in mid-June 2018. Both sources of the bridge cross-section survey were taken into consideration to determine the river geometry features of this region.

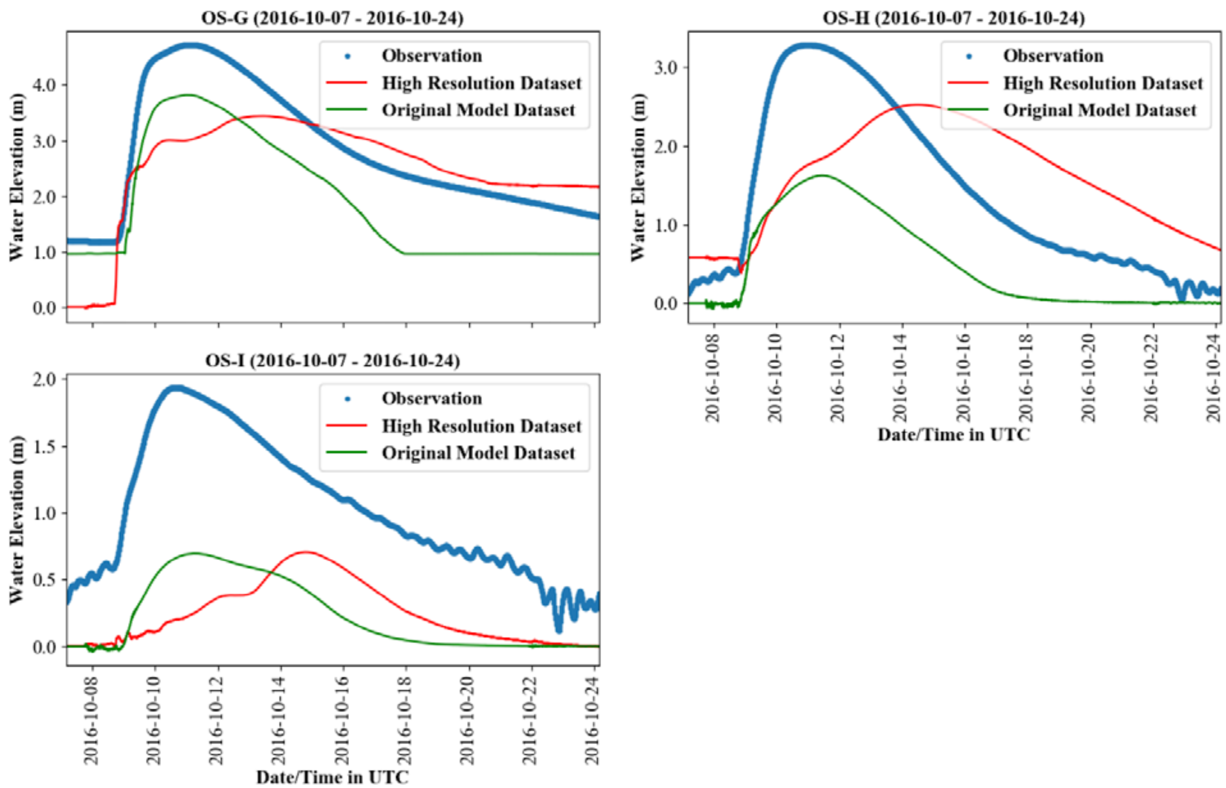

Figure 16. Model output for Hurricane Matthew before and after the high resolution inputs was implemented at USGS stations OS-G, OS-H, and OS-I

Since the rainfall data is a critical input to the model, before making further changes to the model parameters as part of the calibration work, first the quality of the TRMM gridded rainfall data was verified. This was accomplished by running the model with gauged rainfall data obtained from NOAA. First the data quality collected from the available NOAA gauges (12 NOAA gauges) was investigated. This step was also taken to verify that significant runoff volume was not missed. Figure 17 shows the collected cumulative rainfall data at each of the 12 NOAA gauges. There were some gauges that did not match the trends of their neighboring gauges. In significant rainfall events, such as Hurricane Matthew, sudden flat lines result in this cumulative rainfall data that typically means a gauge was non-operational for that period. Gauge RG-I appears not to have been operational until after the main event passed, after comparing this gauge's cumulative rainfall to another gauge in close proximity (RG-D). The first value for the gauge RG-I was on October 9, 2016. At this time, Gauge RG-D had received over 150mm while RG-I was dry. Gauge RG-H appears to have failed right before the main storm hit, as shown in Figure 17 with the flat line in the graph. Gauge RG-K had one of the largest rainfall totals, though it also dropped its signal for a short period near the end of the event. If this rainfall dataset was used as is, it would likely add errors and uncertainty to the model output, as this dataset was used to generate the gridded rainfall data for Hurricane Matthew using the IDW methods available with the TUFLOW model. This issue was solved by excluding gauges RG-I, RG-J, and RG-K and only using the data from the nearby gauges RG-D, RG-L, and RG-G, respectively. Because there was no nearby gauge to RG-H, its data was substituted with the gauge RG-C. After applying these changes, a significant improvement was noticed to the modeled hydrographs at the USGS stations OS-G, OS-H, and OS-I. This significant improvement strongly suggests that the gridded rainfall data generated from using the IDW interpolation method with the gauged rainfall data provides a better representation of the rainfall than using the TRMM data. This could be due to the finer temporal resolution (~20 min) and spatial resolution (500 x 500 m) used with the generated gridded rainfall data. Figure 18 shows the selected NOAA gauges with the hyetographs used for Hurricane Matthew for the rest of the calibration process. Most of the rainfall volume were recorded at 4 NOAA gauges (RG-B, RG-C, RG-G, and RG-H), which are located mainly on the eastern half of the study domain.

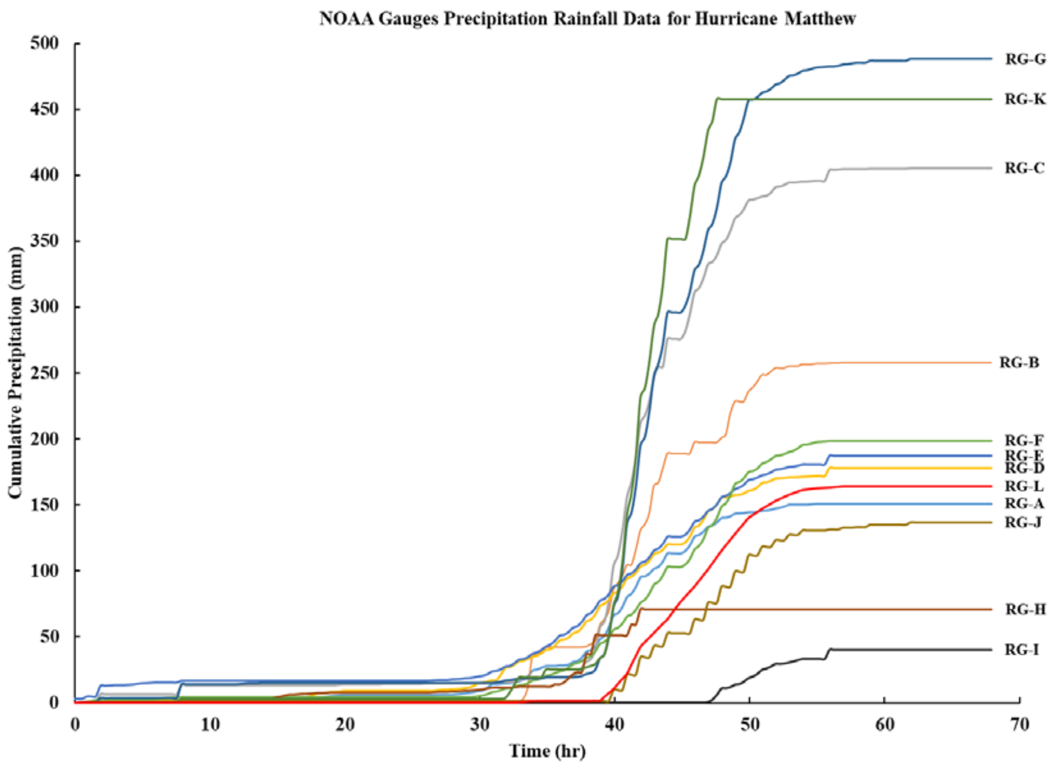

Figure 16. Cumulative rainfall data at each of the 12 NOAA gauges for Hurricane Matthew (2016)

After validating the rainfall data, the hydraulic features were fine-tuned (e.g., the streamflow line width) and parameters (e.g. Manning's coefficient) in the study domain to have a better calibrated model. The main streamflow line widths were adjusted based on the available imagery data. This imagery data was also used to judge the Manning's coefficient values around the USGS stations that had model outputs incommensurate with the observations. Regarding the Manning's coefficient values used, it was noticed that these values were excessively high and much higher than industry standards for some of the land covers. Because of the large domain of the study area, it was impractical to conduct a site visit to the entire area. However, a combination of the highly accurate available land cover, and imagery data and photos available from Google Maps was used to adjust the Manning's coefficient values appropriately. The new Manning's coefficient values were used, which are recommended by the TUFLOW model developers (Brisbane City Council, 2018). After several runs with adjusting the Manning's coefficient values, Table 4 shows the final Manning's coefficient values used in the calibrated model.

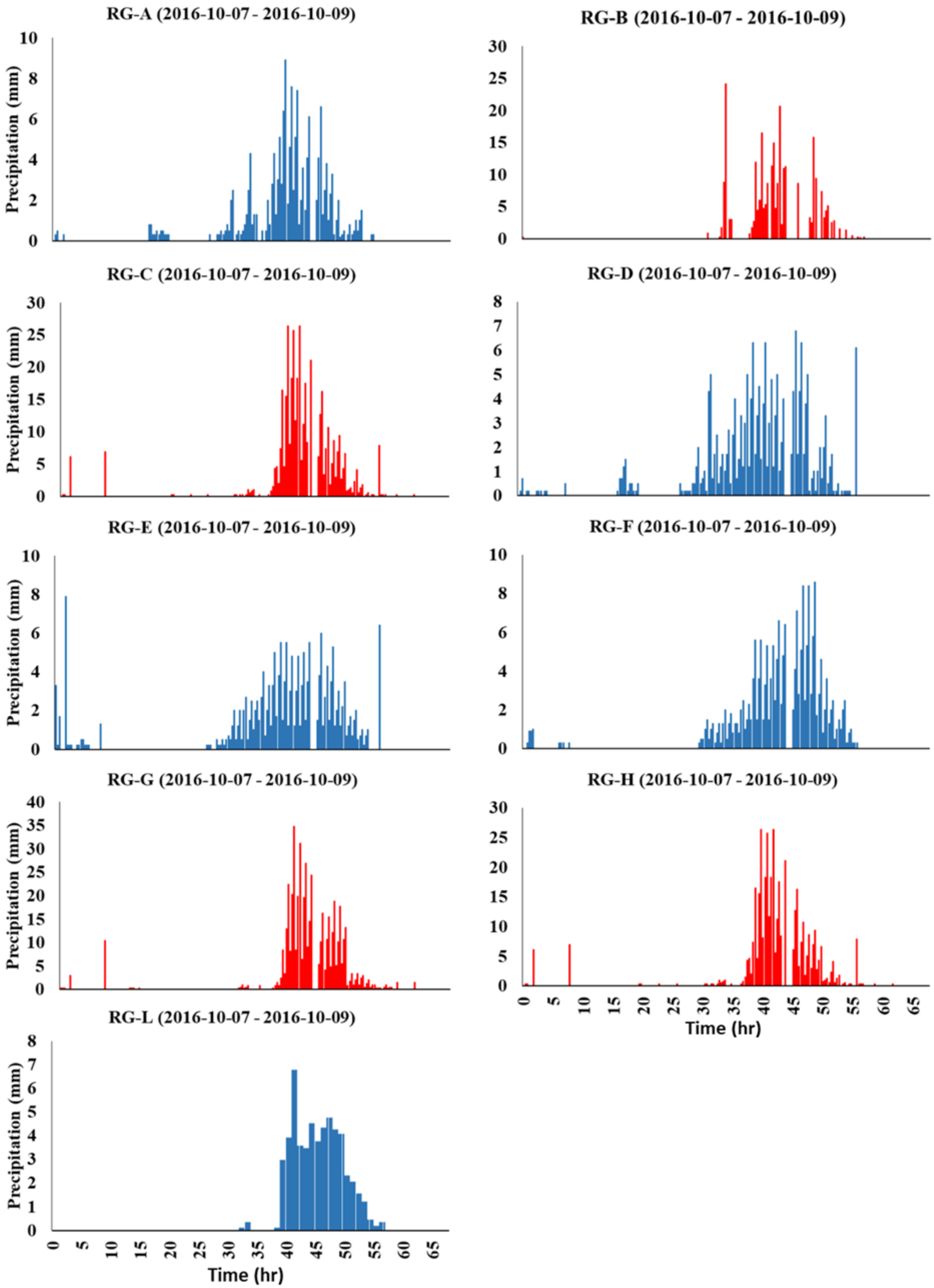

Figure 18. The selected NOAA gauges with the hyetographs used for Hurricane Matthew (2016)

Table 4. Modified Manning's coefficients values for Different Land Cover Types based on the calibration process

Land Cover Code	Land Cover Description	Manning's Coefficient (n)
11	Waterbody	0.035
21	Developed, open space	0.040
22	Developed, low intensity	0.068
23	Developed, medium intensity	0.068
24	Developed, high intensity	0.040
31	Barren land	0.011
41	Deciduous forest	0.12
42	Evergreen forest	0.10
43	Mixed forest	0.15
52	Shrub/srcub	0.15
71	Grassland/herbaceous	0.12
81	Pasture/hay	0.10
82	Crop/vegetation	0.10
90	Woody wetlands	0.086
95	Emergent herbaceous wetlands	0.15

The model was rerun after each enhancement of the hydraulic features and parameters until an acceptable match was found between the modeled and observed stage depth (see Figures 18-a and 18-b). Figures 19 and 20 show an excellent fit with observations at all USGS stations with a maximum difference of about 0.5m between the observed and modeled stage depth hydrographs. The initial water level from the current version of the model is much closer to the observed initial and final water levels. The overall trend of the stage depth hydrographs generated from the calibrated model showed a better match with the observations, especially for the USGS stations OS-G, OS-H, and OS-I.

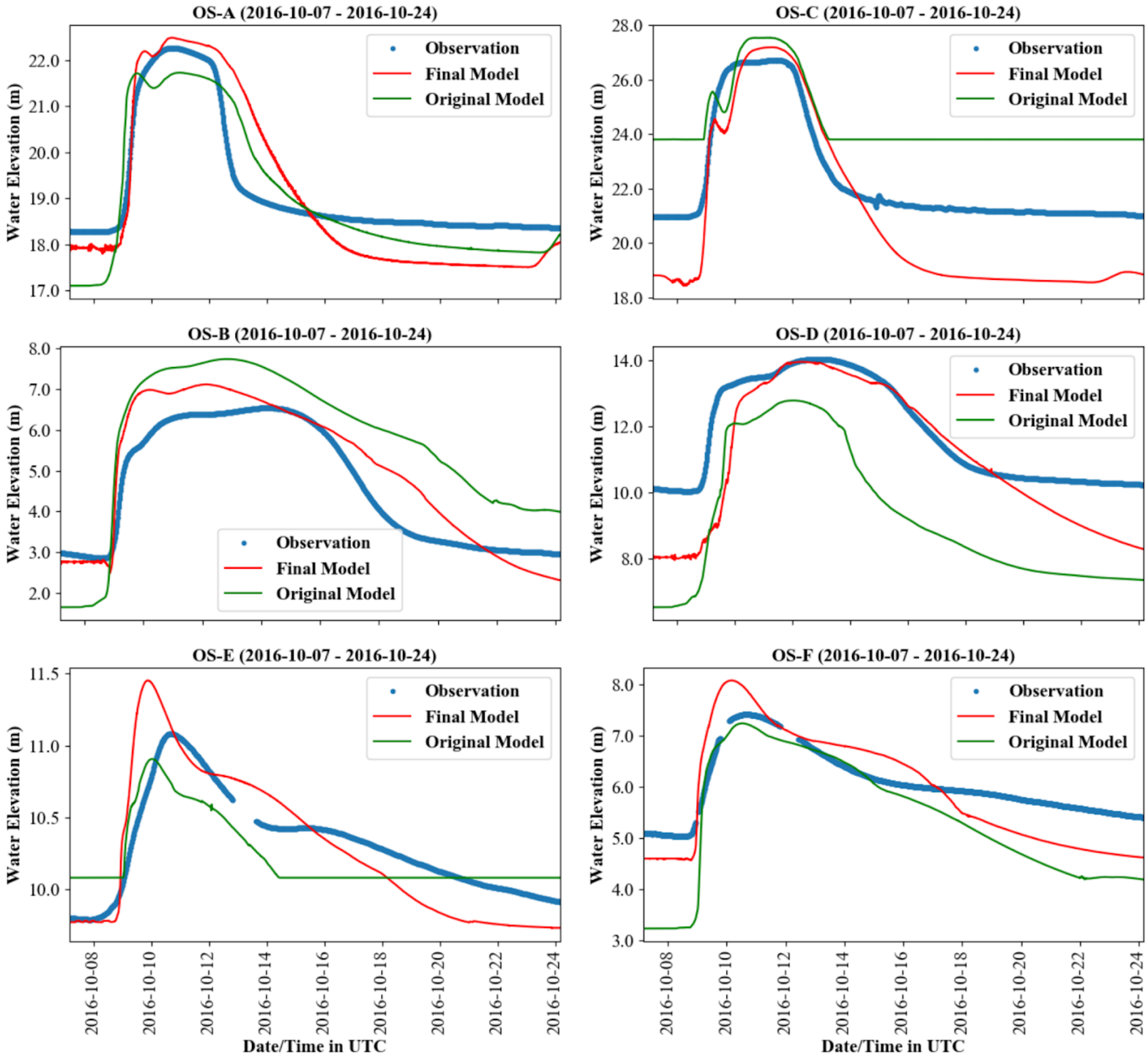

Figure 19. Final model output for Hurricane Matthew at USGS stations OS-A, OS-C, OS-B, OS-D, OS-E, and OS-F

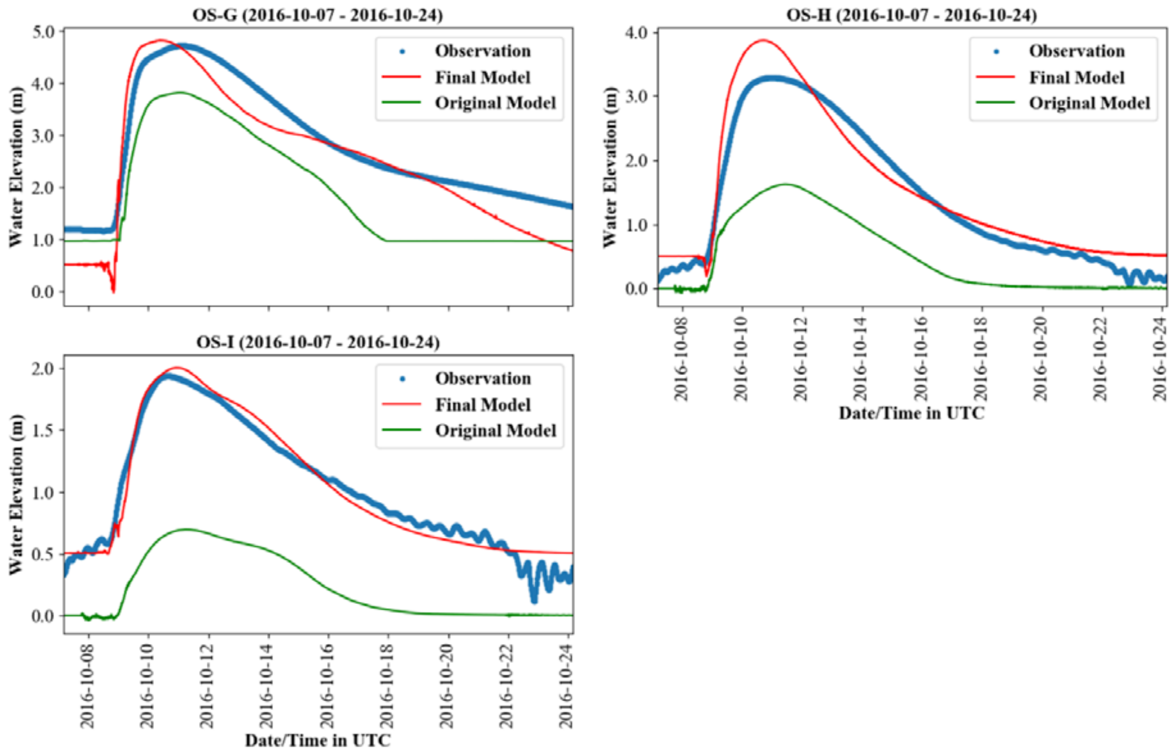

Figure 20. Final model output for Hurricane Matthew at USGS stations OS-G, OS-H, and OS-I

For bridge management purposes during flooding events, the calibration process was specifically conducted so that the modeled stage depths would match the observed stage depths. At the same time, the flow rate simulated at bridge locations was also considered so that it can be used for other future studies and so that it provides more confidence in the model's accuracy. Therefore, a second evaluation check was conducted by comparing the modeled flow rate at the USGS stations with the USGS observations. Figures 21 and 22 show the match of the modeled flow to the observed flow rate hydrographs. At the majority of the USGS stations, the modeled flow rate shows a good match with the observed flow rate (i.e., OS-A, OS-C, and OS-D). However, the peak flow rate simulations at a few of the USGS stations (OS-B, and OS-E) show about 20 to 60 m^3/s difference to the observations with relative error of -20.15% and 110.72% respectively. Sometimes these differences in the peak flow could be due to the model computational cell resolution. To generate the modeled flow rate hydrographs, a line across the desired location was defined to aggregate the flow rate within the computational cells that were covered with this defined line. At some points due to the resolution of the model (30 m), the exact flow pass was not obtained at the desired cross section. The flow rate simulation for USGS stations shown in Figure 20 shows the flow rate simulation for the USGS stations located at the Blackwater River at the east portion of the model. The hydrographs were ordered from the upstream to downstream of the Blackwater River with the first station of OS-E and the last station of OS-I. Other than station OS-E, the modeled flow has an acceptable match with the observed flow for all of the USGS stations. The modeled flow rate hydrograph at OS-E matches the observed hydrograph for the rising and recession limbs, until a specific point. At this point, a higher spike was shown of the flow compared to the observations. Overall, however, the model provides fairly accurate results for the calibration of such a large region, especially given the challenges involved in working with a 2D model.

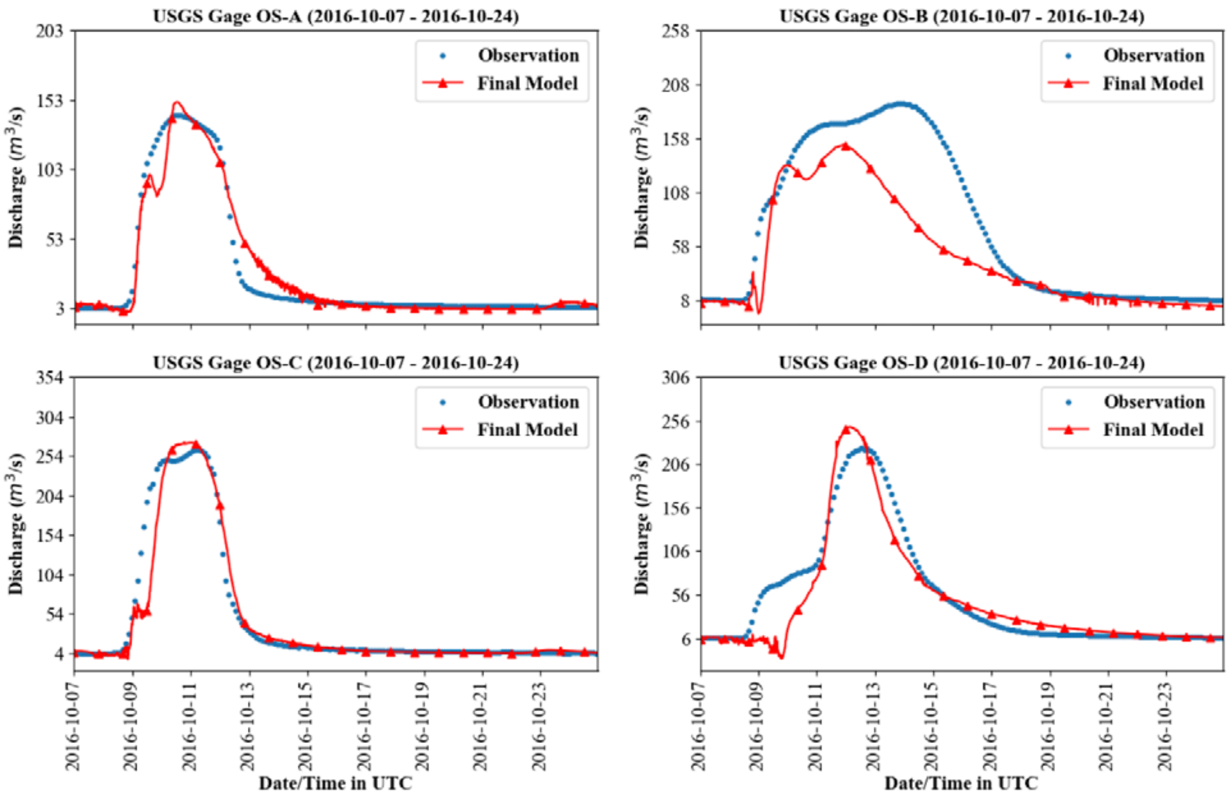

Figure 21. Final model flow output for Hurricane Matthew show higher peaks than the observations at USGS stations OS-A, OS-B, OS-C, and OS-D

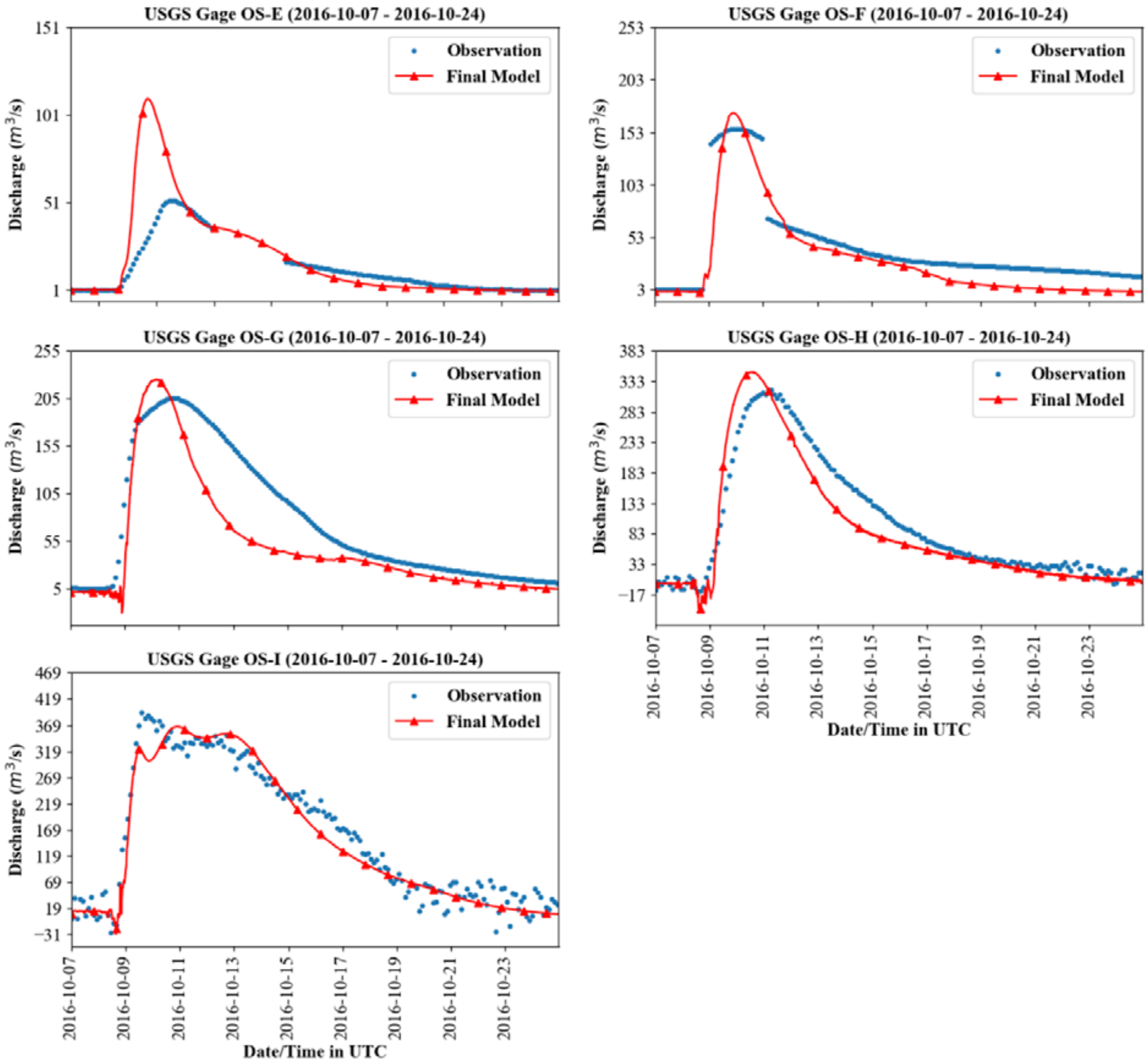

Figure 22. Final model flow output for Hurricane Matthew show good matching to the observations at USGS stations OS-E, OS-F, OS-G, OS-H, and OS-I

Task 3: Workflow Automation

Figure 23 shows the design of the automated workflow for the cloud-based flood warning system. This system uses three AWS resources: (i) A low cost EC2 t2.micro instance running a Linux operating system, (ii) An EC2 G2 or P2 instance with a Windows operating system, and (iii) A S3 Bucket. The EC2 t2.micro instance has two roles in the workflow. First, the instance continuously monitors rainfall forecasts to identify an extreme weather event. When an extreme weather event is identified, the EC2 t2.micro instance starts the EC2 G2 or P2 instance and a model run is initiated. Second, the EC2 t2.micro instance serves the webpages used to visualize and disseminate the model results computed by the larger EC2 G2 or P2 instance. The EC2 G2 or P2 instance includes all of the model components. The EC2 G2 or P2 instance retrieves, preprocesses, prepares the forecast rainfall data and the NWM data, and executes the 2D hydrodynamic model. After the model runs, the EC2 G2 or P2 instance sends model outputs to the EC2 t2.micro instance for visualization and dissemination. The pre-processed inputs, rainfall and boundary condition data, and the model outputs are also sent to the S3 bucket for archiving and reproducibility purposes.

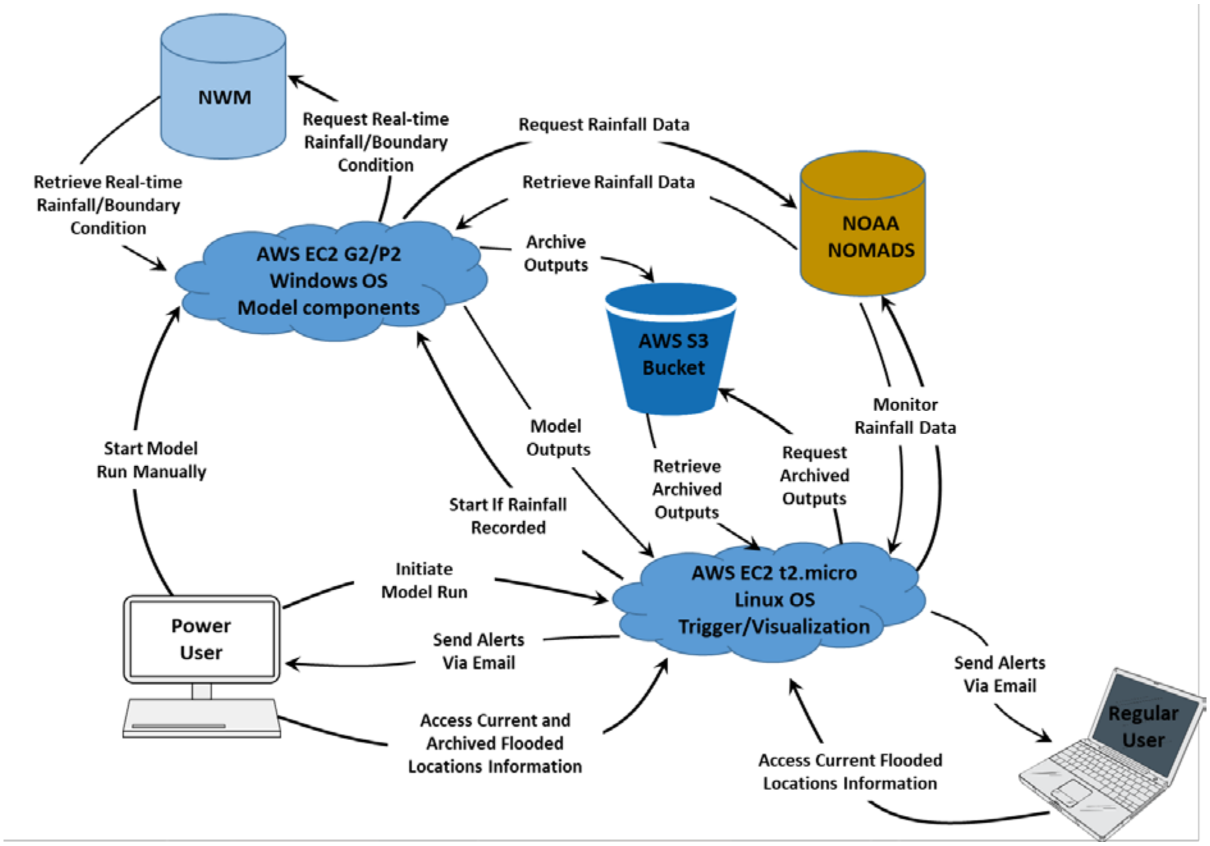

Figure 23. Design of the automated workflow for flood warning model using AWS resources

There are two classes of users that can access the model outputs via the web application running on the EC2 t2.micro instance: regular users and power users. Regular users can access the current flooded locations and can register to receive alerts via email whenever locations are forecast to flood. In the current implementation, regular users do not need to authenticate with the system. Power users have more privileges than regular users, including access to all the archived inundation maps from the S3 bucket and the ability to run the model at any time via a powershell script or through the website hosted by the t2.micro instance.

The main application in the web framework runs on the EC2 t2.micro instance. Code was added to this script for monitoring and accessing the other EC2 G2 or P2 instance. In this code, a process is run every hour to check the HRRR rainfall data (which is updated hourly). If the rainfall is over a certain threshold value, the code will start the EC2 G2 or P2 instance that includes the hydrologic model. Then the EC2 t2.micro instance keeps monitoring the EC2 G2 or P2 instance to make sure that it is fully started. Then the EC2 t2.micro instance initiates a batch file on the EC2 G2 or P2 instance that runs the main workflow for retrieving the data, executing the model, and generating the output (Figure 24). The 2D hydrologic model takes about 10 minutes to run using model grid resolution of 50m (Morsy et. al, 2017). The 2D hydrologic model takes about 38 minutes to run using the model grid resolution of 30m. The model running time is varied based on the number and type of the used GPUs.

Batch File

- **Retrieve and process the latest forecasted rainfall data**
- **Run the models**
- **Generate KMZ file**
- **Send the KMZ file to the EC2 t2.mirco instance**
- **Send the KMZ file and the processed rainfall data to the S3 Bucket.**
- **Generate log file**
- **Send the log file to the EC2 t2.micro instance.**
- **Send the log file to the S3 Bucket.**
- **Delete any generated file from executing the model.**

Figure 24. The structure of the batch file that is responsible for running the whole workflow automatically

This batch file automates the model execution and operates as follows. First, the HRRR data is retrieved and processed. Then, the real-time rainfall and boundary condition data is retrieved from the NWM and processed. Once the input data is retrieved and is available for the 2D model, the model is run and the maximum water level at each computational cell within the study area is computed and recorded for the duration of the simulation period. Once the maximum water level output file is available, a KMZ file is generated from the model output file. This KMZ file includes the following: 1) information about each bridge and culvert provided by VDOT, 2) the maximum water level predicted by the model, and 3) by how much each bridge would be overtopped. The KMZ file is sent to the t2.micro instance to be used for visualization on the website. A log file is generated that includes a record of the parameters and scripts used in the whole process as a reference for users or decision makers. This is helpful to record any errors that could happen while running the workflow. The log file is sent to both the EC2 t2.micro instance and the S3 Bucket for archiving. Finally, any files generated from running the whole workflow are deleted to minimize the storage on the EC2 G2 or P2 instance.

Figure 25 shows the architecture of the current system's website. On the main view, the website contains a navbar allowing the selection of which data to view, a link to the log file, a login page, and a page to register for email alerts. The Google Maps JavaScript Application Programing Interface (API) was used to easily display an accurate and up to date base map along with bridge condition forecasts. When a user clicks on a marker signifying a bridge, they are presented with a box containing more information about that bridge and potential flooding events. Users can sign up for flood alerts. The application will detect when flooding is possible and send an email to everyone registered. Through the website, power users can display output data archived in the AWS S3 bucket without having to store output in the t2.micro instance, which has a limited amount of storage. The power user also can initiate a model run anytime as a second option to run the system as an alternative to the power shell script.

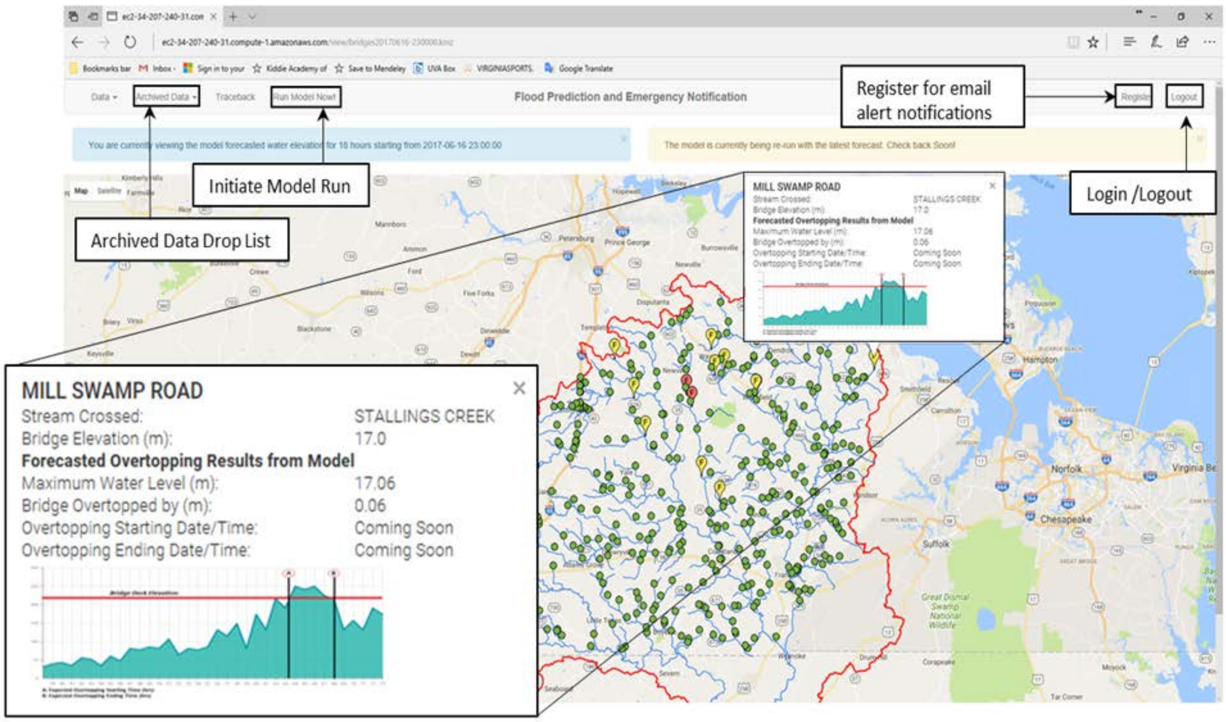

Figure 25. EC2 t2.micro instance and the web framework used to build up the website (Morsy et al., 2018)

The system was designed to be transferable to any cloud computing provider that has better services or prices. The system can also be run on-premises instead of in the cloud if resources are available and security is a concern. Several cloud computing providers were compared and it was found that Google Cloud Platform (GCP) best met the needs of the project. While comparing cloud services, it was found that GCP provided additional benefits over AWS in a couple of key areas. The first key area and biggest benefit is cost. The cost for one hour of the model instance on GCP was around $4.50, which was cheaper than the AWS GPU machine ($8.70/hr) at the time. Additionally, AWS has slower GPUs than GCP. At the time of experimentation, AWS charged a full hour of compute time whenever a machine was started. For the short model runs this led to paying for a lot of computing time that was not used. GCP, however, only charges to the nearest minute. GCP allows full customization of the technical specifications of the instances. This allowed the team to specify an instance with the high-performance GPUs necessary for the model run but not to waste resources on CPUs and Memory. The second key area is the implementation. The GCP ecosystem is also very integrated within itself and allows for easy API calls between instances. This allowed the transfer of data between compute resources to be easier and more secure. While all of these benefits point towards GCP being a better solution at the time of experimentation, the cloud computing market is rapidly growing with each competitor changing their feature sets daily. The solution was designed to be platform independent to allow it to be run on the best available option.

A Version 2 web application has been created which is based on a ReactJS single page application and replaces the KMZ files with a PostgresSQL database to store model results at each VDOT structure location (VFIS, 2018). During this enhancement, a water stage time series was generated at each bridge location in the study area rather than just relying on the maximum water elevation raster. This will allow the system to track exactly what is happening at each bridge location. This V2 web application will provide a much faster and more user-friendly experience. This will also allow the team to expand the system with more statistical analysis and assessment studies to compare the system forecast with the real events. This new web interface will also allow for comparison between the different available options for flood forecasting (e.g., national vs regional flood forecasts) to better inform decision makers.

CONCLUSIONS

- *The quality of the input data, in particular topography, bathymetry, rainfall, and surface roughness, has significant impact on the model calibration process and model performance.*

- *Conducting site visits and surveying stream cross-sections, rather than relying solely on remotely sensed LiDAR data, was very important in improving the model accuracy, especially for the lowest-relief regions.*

- *The calibrated models shows a good match for the observed water elevation and flow at most of the observation stations*. After the calibration process, relative error was within the range of -0.6% to 17.6% between the observed and modeled water surface elevation. However, the eastern-portion of the watershed, which has very flat terrain, remains the most difficult region to model accurately.

- *Even with the efforts to speed up the model and advancements in currently available GPUs, a big challenge of the calibration process remains the model run time. For Hurricane Matthew, which was a 430 hour simulation period, the model takes on average 10 hours to run using the current available high-end GPUs*. This limits the number of different scenarios that could be tested during the calibration process.

- *Using the available cloud computing resources, an automated end-to-end flood warning system (i.e., from forecasts to projected bridge impacts) was designed and built with a customized website to support decision makers in near real-time.*

RECOMMENDATIONS

As this report was being finalized in the spring of 2019, the Governor and the Virginia General Assembly determined that coordinated state agency research activities in the areas of climate change, sea level rise in coastal areas, roadway flooding due to storm surge, and roadway management strategies in flooding events are desirable. The Department of Natural Resources has been identified as the lead agency for these initiatives. This study's recommendation therefore reflects that new interagency approach.

1. *The Virginia Transportation Research Council should brief the executives in the Department of Natural Resources (DNR) on the work accomplished to date on the R^2S^2 model.* The briefing should include the capabilities of the current model, its current limitations, and potential modifications that could improve the model.

IMPLEMENTATION AND BENEFITS

Implementation

Recommendation 1 will be implemented by the VTRC Deputy Director of Research in fy20. The Chief Resiliency Officer and/or the Special Assistant to the Governor for Coastal Adaptation in DNR will be contacted about a potential meeting date to discuss the R^2S^2 model as a tool to forecast potential flooding impacts in real-time for roadway management responses in coastal areas. If appropriate, the discussion can also include a discussion of additional efforts which would further test the model's accuracy and/or expand the model to additional regions of Virginia.

If additional effort is warranted as a result of the discussion with DNR, the ways in which R^2S^2 could be improved include the following : (1) develop system enhancements to provide longer-range forecasting (i.e., 3-5 days vs. 18 hours) of flooding impacts to anticipate potential impacts of major storm events such as hurricanes further in advance; (2) include additional bridge cross-section data and river bathymetry when available in the coastal study region to improve the model accuracy, especially in the easternmost portion of the study area that has very low relief terrain; (3) provide additional model evaluation using VDOT records of bridge and culvert road closings due to flooding in the coastal study region. Other potential R^2S^2 enhancements include making use of river forecasting information from the National Water Model, and exploring the possibility of flash flood forecasting for small catchments that are flood prone.

Benefits

If the R^2S^2 flood warning system is judged to be worthy of implementation by DNR, VDOT officials and potentially local public works officials in much of the Hampton Roads District could be provided with advance information on forecasted flooding impacts to bridges and culverts. This information can be used for road and bridge closure decisions, ultimately increasing driver safety during storm events. For VDOT, use of the R^2S^2 model could also allow improved prioritization of the use and timing of limited VDOT maintenance resources and would provide VDOT and coastal localities with additional time to plan for major storm events.

ACKNOWLEDGMENTS

The Regional River Severe Storm (R^2S^2) model was originally built by Hassan Water Resources, PLC, in collaboration with VDOT's Hampton Roads District Hydraulics Engineer Andrew B. Scott. This project greatly benefited from both data and insights that resulted from this prior work. This work also would like to acknowledge the Viz Lab, a facility for University of Virginia students, staff, and faculty to explore and investigate the power of visualization in research and education, for providing the research team with a local machine with GPUs to test the design and perform runs before moving the system to the cloud.

REFERENCES

Brisbane City Council. Manning's Roughness, 2018. https://www.brisbane.qld.gov.au/sites/default/files/ncd_appendixc_part3.pdf. Accessed November 26, 2018.

Caviedes-Voullième, D., García-Navarro, P. and Murillo, J. Influence of mesh structure on 2D full shallow water equations and SCS Curve Number simulation of rainfall/runoff events. *Journal of Hydrology*, 448, 2012, pp.39-59.

Cobby, D.M., Mason, D.C. and Davenport, I.J. Image processing of airborne scanning laser altimetry data for improved river flood modelling. *ISPRS Journal of Photogrammetry and Remote Sensing*, Vol. 56, No. 2, 2001, pp.121-138.

Galarneau Jr, T.J., Davis, C.A. and Shapiro, M.A. Intensification of Hurricane Sandy (2012) through extratropical warm core seclusion. *Monthly Weather Review*, Vol. 141, No. 12, 2013, pp.4296-4321.

Horritt, M.S., Bates, P.D. and Mattinson, M.J. Effects of mesh resolution and topographic representation in 2D finite volume models of shallow water fluvial flow. *Journal of Hydrology*, Vol. 329, No. 1-2, 2006, pp.306-314.

Huxley, C. and Syme, B. TUFLOW GPU-Best practice advice for hydrologic and hydraulic model simulations. *In 37th Hydrology & Water Resources Symposium 2016: Water, Infrastructure and the Environment*. Engineers Australia, 2016, pp. 195.

Kalyanapu, A.J., Burian, S.J. and McPherson, T.N. Effect of land use-based surface roughness on hydrologic model output. *Journal of Spatial Hydrology*, Vol. 9, No. 2, 2010, pp.51-71.

Kates, Robert William, et al. "Reconstruction of New Orleans after Hurricane Katrina: a research perspective." *Proceedings of the national Academy of Sciences*, 103.40 (2006): 14653-14660.

Kates, R.W., Colten, C.E., Laska, S. and Leatherman, S.P. Reconstruction of New Orleans after Hurricane Katrina: a research perspective. *Proceedings of the National Academy of Sciences*, Vol. 103, No. 40, 2006, pp.14653-14660.

LeVeque, R.J. *Finite volume methods for hyperbolic problems*. Cambridge University Press. Vol. 31, 2002.

Maidment, D.R. Conceptual framework for the national flood interoperability experiment. *JAWRA Journal of the American Water Resources Association*, Vol. 53, No. 2, 2017, pp.245-257.

Marks, K. and Bates, P. Integration of high -resolution topogr
models. *Hydrological Processes*, Vol. 14, No. 11 -2122, 2000, pp.2109

Morsy, M.M., Goodall, J.L., O'Neil, G.L., Sadler, J.M., Voce, D., Hassan, G. and Huxley, C. A cloud-based flood warning system for forecasting impacts to transportation infrastructure systems. *Environmental Modelling & Software*, Vol. 107, 2018, pp.231-244.

Morsy, M.M., O'Neil, G.L., Goodall, J.L. and Hassan, G. Computational Enhancements for the Virginia Department of Transportation Regional River Severe Storm (R2S2) Model. *Virginia Transportation Research Council*, No. FHWA/VTRC 17-R18, 2017.

Next Generation Weather Radar. NEXRAD, 2018. https://www.ncdc.noaa.gov/data-access/radar-data/nexrad. Accessed November 26, 2018.

Nicholls, R.J. and Cazenave, A. Sea-level rise and its impact on coastal zones. *Science*, Vol. 328, No. 5985, 2010, pp.1517-1520.

Nicholas, A.P. and Mitchell, C.A. Numerical simulation of overbank processes in topographically complex floodplain environments. *Hydrological Processes*, Vol. 17, No. 4, 2003, pp.727-746.

Refsgaard, J.C. Parameterisation, calibration and validation of distributed hydrological models. *Journal of Hydrology*, Vol. 198, No. 1-4, 1997, pp.69-97.

Sadler, J.M., Goodall, J.L., Morsy, M.M. and Spencer, K. Modeling urban coastal flood severity from crowd-sourced flood reports using Poisson regression and Random Forest. *Journal of Hydrology*, Vol. 559, 2018, pp.43-55.

Schreider, S.Y., Smith, D.I. and Jakeman, A.J. Climate change impacts on urban flooding. *Climatic Change*, Vol. 47, No. 1-2, 2000, pp.91-115.

Suarez, P., Anderson, W., Mahal, V. and Lakshmanan, T.R. Impacts of flooding and climate change on urban transportation: A systemwide performance assessment of the Boston Metro Area. *Transportation Research Part D: Transport and Environment*, Vol. 10, No. 3, 2005, pp.231-244.

Syme, W.J. TUFLOW-Two & One dimensional unsteady flow Software for rivers, estuaries and coastal waters. *In IEAust Water Panel Seminar and Workshop on 2d Flood Modelling*, Sydney, February 2001.

United States Geological Survey. National Hydrography, 2018. https://www.usgs.gov/core-science-systems/ngp/national-hydrography. Accessed November 26, 2018.

Virginia Flood Information System. VFIS, 2018. https://vfis-beta.uvahydroinformatics.org/. Accessed November 26, 2018.

Virginia Geospatial Services. Land Cover, 2018. https://www.vita.virginia.gov/integrated-services/vgin-geospatial-services/land-cover/. Accessed November 26, 2018.

Virginia LIDAR. Elecation – LIDAR, 2018. https://www.vita.virginia.gov/integrated-services/vgin-geospatial-services/elevation---lidar/. Accessed November 26, 2018.